POLITECNICO DI TORINO

Master of Science in Energy and Nuclear Engineering

Master Thesis

Optimisation of the Energy Management System of a parallel Hybrid Electric Vehicle

Supervisors:

Prof. Luciano Rolando

Candidate:

Miriana FRATINO

December 2020

Abstract

Legislations worldwide are focusing on the achievement of significant abatements of pollutants and GHG emissions from the transportation sector. Hybrid electric vehicles are considered a promising solution to achieve a sustainable transportation system in the near future. However, their potential can be fully exploited by only means of an ad hoc energy management system, capable of achieving an optimal partition between the different power sources available on board of the vehicle. Consequently, the aim of this thesis is the definition of a procedure to design an optimal powertrain control strategy for a P2 Plug-in Hybrid Electric Vehicle (PHEV). Starting from the problem formulation, the ideal performance of the vehicles will be analysed through a global optimisation algorithm in order to point out information which can be used to define new control laws to integrate in Rule Based strategy adopted by the manufacturers.

Index

Abstract I

Symbols V

Definitions VII

List of Tables XI

List of Figures XIII

1 Introduction 1

1.1 Role of the road transport sector 3

1.1.1 Potential of Electric Powertrain 4

1.2 Emission Legislations 7

1.2.1 Regulation on air pollutant emissions 7

1.2.2 Regulation on GHG emissions 8

1.3 Driving Cycles 10

1.3.1 NEDC 10

1.3.2 WLTC 11

1.3.3 RDE 14

2 Hybrid Electric Vehicles 16

2.1 Hybrid Electric Vehicles 16

2.1.1 Hybridization levels 16

2.1.2 Hybrid Architectures 18

3 Control Strategies for Hybrid Vehicles 25

3.1 Energy Management in HEVs 25

3.2 Problem Formulation 26

3.3 Control strategies 26

3.4 Dynamic Programming 28

3.4.1 General concepts 28

4 Modelling Approach 32

4.1 Introduction 32

4.2 Backward Kinematic Analysis 32

4.3 Quasi-Static Analysis 34
4.4 Forward Dynamic Analysis 34
4.5 Powertrain modelling 35
4.5.1 Engine 35
4.5.2 Electric Machine 37
4.5.3 Battery 37
4.6 Equations of motion 38
4.7 Modelling Tools 39
5 Case studies 42
5.1 Test case 42
5.2 Experimental Campaign 43
5.3 GT-SUITE embedded Dynamic Programming 45
5.3.1 Model Setup 45
5.3.2 Model validation 45
5.3.3 Dynamic Programming implementation 47
5.4 Results 52
5.4.1 NEDC & WLTC 52
5.4.2 RDE 63
6 Conclusions 67
Acknowledgement 69
Bibliography 71

Symbols

APU:	Auxiliary Power Unit
BMEP:	Brake Mean Effective Pressure
BSFC:	Brake Specific Fuel Consumption
CFD:	Computational Fluid Dynamic
CD:	Charge Depleting
CS:	Charge Sustaining
DP	Dynamic Programming
EAP:	Extensible Authentication Protocol
ECU:	Electronic Control Unit
ECMS:	Equivalent Consumption Minimization Strategy
EEA:	European Environment Agency
EM:	Electric Machine
EMS:	Energy Management System
ETS:	Emission Trading System
EU:	European Union
EV:	Electric Vehicle
GHG:	Greenhouse Gas
GDP:	Gross Domestic Product
HEV:	Hybrid Electric Vehicle
ICE:	Internal Combustion Engine
IPCC:	Intergovernmental Panel on Climate Change
LDV:	Light Duty Vehicle
MGU:	Motor Generator Unit
NEDC:	New European Driving Cycle
OEM:	Original Equipment Manufacturer
PID:	Proportional-Integrative-Derivative

PHEV:	Plug-in Hybrid Electric Vehicle
RB:	Rule Based
RDE:	Real Driving Emissions
RESS:	Rechargeable Energy Storage System
RPM:	Revolution Per Minute
SOC:	State of Charge
SOE:	State of Energy
TTW:	Tank to Wheel
WLTP:	Worldwide Harmonized Light Vehicles Test Procedure

Definitions

CO_2:	Carbon dioxide
A_f:	Vehicle frontal area
C_o:	Minimum input torque
C_{IN}:	Input torque
C_x:	Aerodynamic drag coefficient
c_{roll}:	Rolling resistance coefficient
E_{batt}:	Total storable energy in the battery
F_t:	Total tractive force at the wheel-road interface
F_x:	Aerodynamic drag
g:	Gravitational acceleration
g_N:	Terminal cost
I:	Current
J:	Cost function of optimal control problem
k:	Time step
L:	Instantaneous cost function
M_{eff}:	Effective vehicle mass
NO_x:	Nitrogen oxides
m_f:	Total fuel consumption
$\dot{m}_{eq}(t)$:	Instantaneous equivalent fuel consumption
$\dot{m}_f(t)$:	Instantaneous fuel consumption (fuel mass flow rate)
$\dot{m}_{ress}(t)$:	Instantaneous virtual fuel consumption
P:	Vehicle weight
P_{batt}:	Battery power
$P_{electric}$:	Electric motor electrical power
P_{mech}:	Electric motor mechanical power

$P_{EL\ GEN}$: Electric generator power

P_{EM}: Electric machine power

P_{eng}: Engine power

P_{ICE}: Internal combustion engine power

$PM_{2.5}$: Particulate Matter 2.5

p_{me}: Mean effective pressure

p_{ma}: Mean analytical pressure

P_{req}: Power requested by the driver

$p(SOC)$: Penalty function

p_k: Penalty fuction

$Q(t)$: Instantaneous charge stored in the battery

Q_{lhv}: Fuel Lower Heating Value

Q_{max}: Maximum battery charge level

$R_{h_{Series}}$: Series hybridisation ratio

$R_{h_{Parallel}}$: Parallel hybridisation ratio

R_s: Rolling resistance

s: Equivalence factor

SOC_0: Initial state of charge

SOC_{des}: Target battery SOC

SOC_f: Final state of charge

SOC_{grid}: Discretised SOC points

t: Time

T_{EM}: Electric Motor torque

T_{ice}: Internal combustion engine torque

T_{loss}: Loss torque

T_{mot}: Electric motor torque

T_N: Terminal State Penalty

u: Control policy

v: Longitudinal vehicle velocity

v_r: Relative vehicle velocity

V:	Voltage
ω_{eng}:	Engine speed
x:	State variable
Y:	Cost-to-go of the tail subproblem
α:	Penalty function exponent
β:	Terminal state penalty exponent
γ:	Terminal state penalty weight
δ:	Road slope
η_{AT}:	Automatic Transmission efficiency
η_m:	Mesh efficiency
η_g:	Engine efficiency
ρ_a:	Air density
ρ_g:	Fuel density
σ:	Curve fitting coefficient

List of Tables

Table 2.1 The main features and capabilities of various hybrid electric vehicles [19]...18
Table 5.1 Detailed test campaign for powertrain characterisation [34]..................44

List of Figures

Figure 1.1 Trends in the main air pollutant emissions and in gross domestic product in the EU-28 [2] 1
Figure 1.2 Air pollutant and greenhouse gas emissions as a percentage of total EEA-33 pollutant emissions in 2017, by sectors [2] 2
Figure 1.3 Fuel efficiency and fuel consumption in private cars, 1990-2015 [2] 3
Figure 1.4 Graphs of the non-ICE models in production and development in 2017 [7] 4
Figure 1.5 Powertrain composition ratio prediction for global light vehicle sales (source: Marklines database) 4
Figure 1.6 Global electric car stock, 2010-19 [8] 5
Figure 1.7 Trends in emissions of air pollutants from transport [9] 6
Figure 1.8 EU greenhouse gas emissions in the transport sector [10] 6
Figure 1.9 Emission limits (g/km) of the successively introduced Euro emission standards for passenger vehicles [12] 8
Figure 1.10 Summary of target levels for cars for 2025 and 2030 [13] 9
Figure 1.11 Divergence between real-world and manufacturers' type-approval CO2 emission values for various on-road data sources, including average estimates for private cars, company cars, and all data sources [11] 10
Figure 1.12 Real Driving Emission features [14] 11
Figure 1.13 Speed profile of the WLTC driving cycles for Classes 1,2 and 3-2; discontinuous line along the Class 3-2 graph shows the Europe NEDC speed/time trace (PMR: power mass ratio) [16] 12
Figure 1.14 Comparison of the speed/acceleration distribution between the WLTC Class 3-2 and the NEDC [16] 12
Figure 1.15 Comparison of the technical specifications between the WLTC and the NEDC driving schedules [16] 13
Figure 1.16 Divergence 'real-world' vs official CO_2 [14] 14
Figure 1.17 Boundary conditions for RDE tests [17] 15
Figure 2.1 The spectrum of vehicle hybridization levels[18] 17
Figure 2.2 Scheme of a series hybrid architecture 19
Figure 2.3 Series Hybridization Level [20] 20
Figure 2.4 Scheme of a parallel hybrid architecture 21
Figure 2.5 Parallel Hybridization Level [20] 21
Figure 2.6 Classification of parallel hybrid according to the EMs position [20] 22
Figure 2.7 Koeninggseg Regera architecture 23
Figure 2.8 Toyota Hybrid System architecture 24
Figure 3.1 Two-layer architecture in a hybrid vehicle [18] 25

Figure 3.2 Arc costs in the simplified example 30
Figure 3.3 Cost-to-go and optimal path in the simplified example........................31
Figure 4.1 Information flow in a backward model for motor vehicles fuel consumption calculation..33
Figure 4.2 Modelling approach of a parallel HEV: (a) forward- and (b) backward-facing models..35
Figure 4.3 Main engine modelling methodologies [30] 36
Figure 4.4 Electrical equivalent model of battery 38
Figure 4.5 Forces acting on a vehicle [12] 39
Figure 5.1 Powertrain schematics and main component [36] 42
Figure 5.2 Powertrain layout with instrumentation details. Voltage and current sensors are used to measure the electrical power exchanged between battery and electric motor; a torque sensor on the propeller shaft measures the total torque coming out from the automatic transmission. The hydraulic pressures in the four brake calipers are measured and CAN data is logged.[16]...................................43
Figure 5.3 Simplified vehicle model 45
Figure 5.4 VehKinemAnalysis Template during validation phase 46
Figure 5.5 SOC during NEDC in the validation phase...46
Figure 5.6 SOC during WLTC in the validation phase...46
Figure 5.7 ICE torque during NEDC in the validation phase 47
Figure 5.8 ICE torque during WLTC in the validation phase 47
Figure 5.9 CO2 consumption in g/km during NEDC 47
Figure 5.10 VehKinemAnalysis Template 49
Figure 5.11 VehStateOptimization Main folder 49
Figure 5.12 State of Charge during NEDC with different values of gamma 50
Figure 5.13 Zoom of State of Charge during NEDC with different values of gamma...51
Figure 5.14 State of Charge during NEDC with different values of beta...............51
Figure 5.15 VKA: Independent Variable Setting...52
Figure 5.16 DP State of charge during (a) NEDC and during (b) WLTC...............52
Figure 5.17 DP power split during NEDC 53
Figure 5.18 NEDC: Map of Optimal Cost To Go 53
Figure 5.19 NEDC: Map Of Optimal Cost To Go without the constraint on the ICE 54
Figure 5.20 NEDC: Urban Driving Cycle 54
Figure 5.21 NEDC: Extra Urban Driving Cycle 55
Figure 5.22 WLTC: Low phase 55
Figure 5.23 WLTC: extra-high phase 56
Figure 5.24 SOC with RDE 57
Figure 5.25 NEDC: SOC trends of Rule Based and DP models 58
Figure 5.26 WLTC: SOC trends of Rule Based and DP models 58

Figure 5.27 NEDC operating modes with (a) Rule Based strategy and (b) DP strategy....59
Figure 5.28 WLTC operating modes with (a) Rule Based strategy and (b) DP strategy....59
Figure 5.29 NEDC power split with (a) Rule based strategy and (b) DP strategy 60
Figure 5.30 WLTC power split with (a) Rule based strategy and (b) DP strategy 60
Figure 5.31 ICE operating points during NEDC obtained with (a) Rule based strategy and (b) DP strategy....61
Figure 5.32 ICE operating points during WLTC obtained with (a) Rule Based strategy and (b) DP strategy....61
Figure 5.33 NEDC: Fuel consumption....62
Figure 5.34 WLTC: Fuel consumption....62
Figure 5.35 NEDC power split: area with ICE on....63
Figure 5.36 RDE vehicle speed....64
Figure 5.37 RDE operating modes with (a) Rule based strategy and (b) DP strategy....64
Figure 5.38 RDE power split with (a) Rule based strategy and (b) DP strategy....65
Figure 5.39 RDE driving cycle analysis....65
Figure 5.40 RDE: Fuel consumption....66

1 Introduction

Climate change is a reality and is already causing phenomena of frequency and intensity never seen in human history. The Intergovernmental Panel on Climate Change (IPCC) confirmed that it is incredibly likely that the increase in greenhouse gas concentrations due to social activities have caused most of the observed changes in the climate system (IPCC, 2013a). Since the persistent environmental and climate challenges at European and global scales, European policymaking is increasingly driven by long-term sustainability goals as embedded in the EU's Seventh Environment Action Programme (7th EAP) 2050 vision, the 2030 agenda for sustainable development and the Paris Agreement on climate change. [1]

Figure 1.1 and Figure 1.2 shows respectively the general trend of the primary air pollutant emissions and gross domestic product in the EU-28 from 2000 to 2017, and the air pollutant and greenhouses gas emissions responsible by sectors.

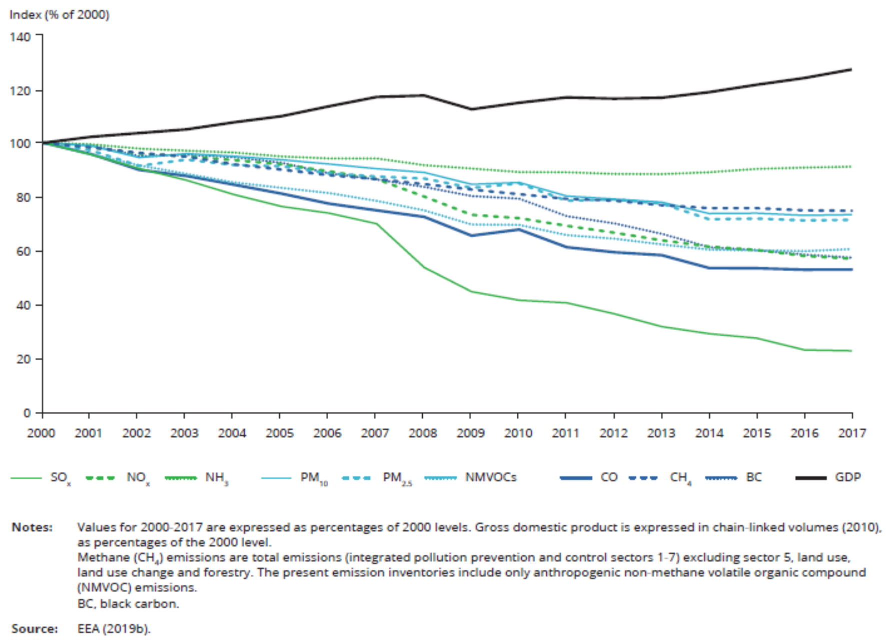

Figure 1.1 Trends in the main air pollutant emissions and in gross domestic product in the EU-28 [2]

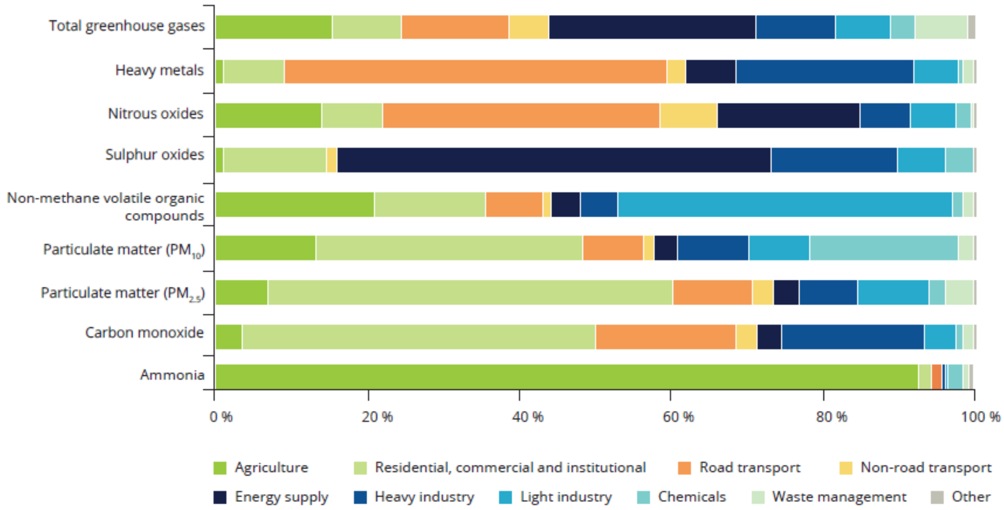

Notes: Heavy metals include arsenic, cadmium, chromium, copper, lead, mercury and zinc and are aggregated by mass. Only those air pollutants covered by the CLRTAP are included.

Sources: EEA (2019g) for total GHGs and EEA (2019f) for air pollutants.

Figure 1.2 Air pollutant and greenhouse gas emissions as a percentage of total EEA-33 pollutant emissions in 2017, by sectors [2]

The reduction of the environmental and climate pressures arising from Europe's transport sector will be critical in achieving the 7th EAP's longer-term objectives since it is one of the key economic sectors. There are high expectations for new passenger vehicle technologies, and increasingly for electric vehicles, to reduce these environmental pressures. Since, historically, passenger vehicles have dominated emissions in the transport sector, and that road vehicles have shorter development times and lifetimes than aircraft, trains and ships. Development and market penetration of new passenger vehicle technologies is, therefore, easier to achieve than for other modes of transport and offers more significant reductions in CO_2 and air pollutant emissions [3].

The role of electrification of the vehicle is pivotal to reach a climate-friendly economy because electrified powertrains, including Electric Vehicles (EVs), Plug-in Hybrid Vehicles (PHEVs) and full Hybrid Electric Vehicles (HEVs), offer the potential for dramatic emission reductions. The object of the analysis of this dissertation is a PHEV. Hybrid vehicles derive part of their advantages from the fact that the total power request can be split among the fuel and the electrical energy buffer. This fact poses some interesting challenges from the control standpoint, since the benefits, that can be achieved through hybridisation, strongly depend from the optimisation of the powertrain control strategy [4].

This thesis work was aimed at developing a procedure to design an optimal powertrain control strategy for a Parallel Hybrid Electric Vehicle. The vehicle under investigation is a Plug-in Hybrid Vehicle that utilises a rechargeable battery that can be restored to full charge by connecting it to an external electric power source. To set the ideal performances for the case study, global optimisation has been used, particularly Dynamic Programming.

1.1 Role of the road transport sector

Emissions from the EU transport sector are not reducing enough to limit its environmental and climate impacts in Europe, it continues to be a significant source of air pollution, despite the introduction of new legislations and the use of cleaner technologies. The reason can be blamed to the increase of car ownership and the distances driven (Figure 1.3) [5][6].

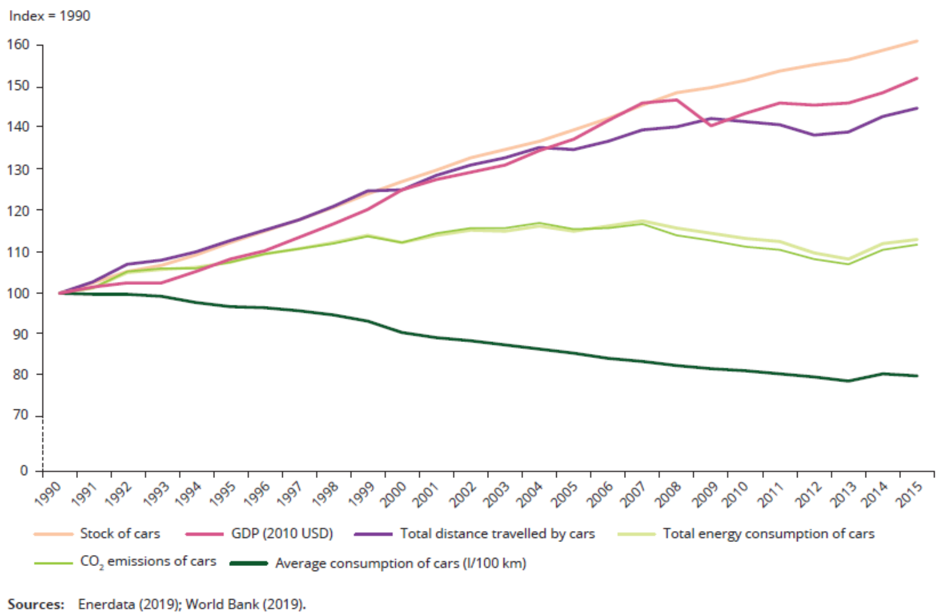

Figure 1.3 Fuel efficiency and fuel consumption in private cars, 1990-2015 [2]

This result highlights the importance of focusing on transforming the whole systems of road transport. In this context, the "Eclectic" represents the principal solution for the near future. Eclectic means that there are a lot of several technical solutions in terms of powertrain development, both the new ICE models and the electrified vehicles, that could live side by side. The market is moving in this direction; many companies in the world are developing new solutions for electrified powertrains, especially Battery Electric Vehicles and Plug-in Electric Vehicles (Figure 1.4).

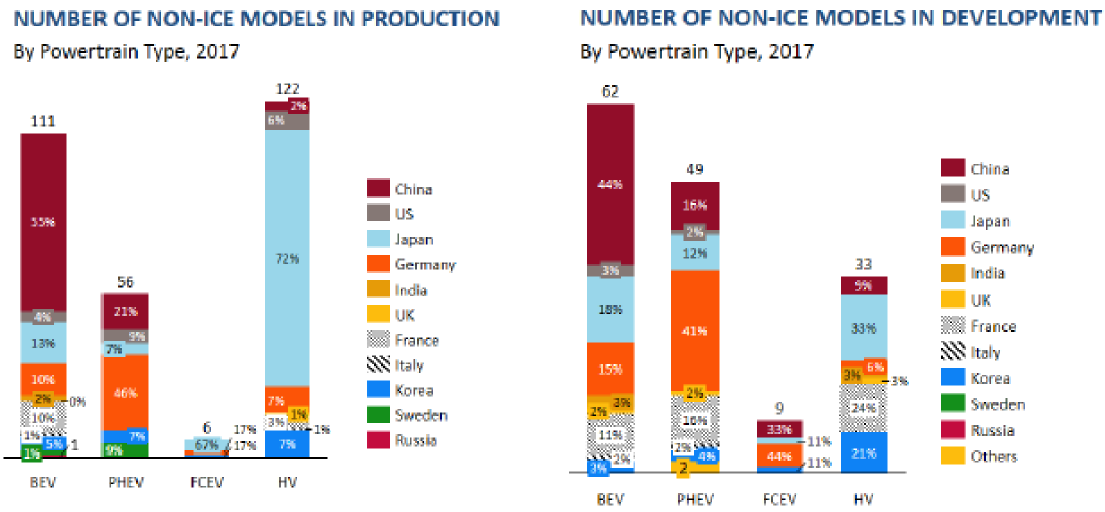

Figure 1.4 Graphs of the non-ICE models in production and development in 2017 [7]

In the expected share of the market in 2032 (Figure 1.5), ICE continues to dominate but with a strong component of electrification.

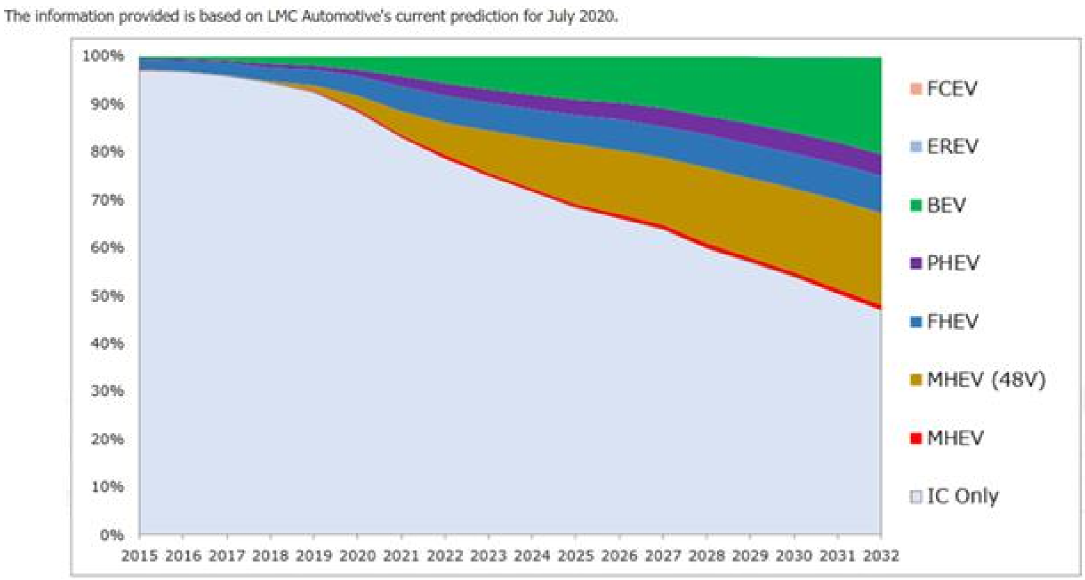

Figure 1.5 Powertrain composition ratio prediction for global light vehicle sales (source: Marklines database)

1.1.1 Potential of Electric Powertrain

The principal benefits of EVs are that they do not produce local emissions, the energy required by electric powertrain can be created by renewable energy sources, and they are characterised by higher efficiency (70%) than ICE (19% gasoline). The drawbacks of Electric Powertrain consist of:

- non-tailpipe emissions: production of emission that could not be avoided even if the vehicle is propelled by a no-emitted motor (from brake wear, tire/road wear and road-dust resuspension):
- although the improvement in battery technology, the typical range of EVs is quite far respect to the conventional ones (average vehicle use is 200 miles/week);
- EVs battery recharge represents a problem due to the request time, the cost and high instantaneous necessary power from renewable sources;
- the price is very high respect to the conventional vehicles.

In this context, HEVs represents the synergies between the Electric Vehicles and the ICE vehicles, they combine the desirable features of EVs with the range capability of conventional vehicles to offer drivers the same range as traditional ICEs but can also lead to the environmental benefits of EVs for short distances. [7] HEV are described in more details in Chapter 2.

The technological development in the European vehicle manufacturing industry was driven by the need to respect the progressively stricter European regulations. The past decades were be characterised by the development of electric and hybrid vehicle technologies (Figure 1.6), eco-innovations, and improvements in conventional engine and exhaust technologies.

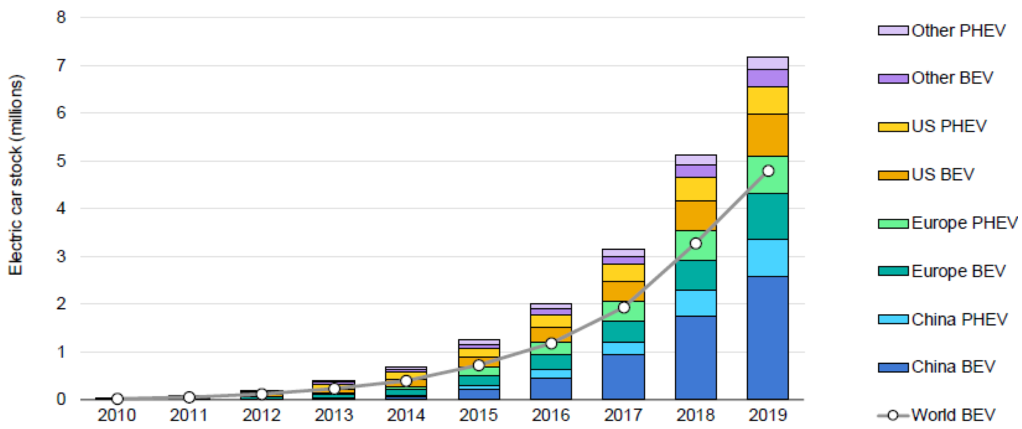

Figure 1.6 Global electric car stock, 2010-19 [8]

It is worth to mention that progress has been made since 1990 in reducing the emissions of many air pollutants from the transport sector (Figure 1.7). Across the EEA-33 (the 28 EU Member States plus Iceland, Lichtenstein, Norway, Switzerland and Turkey) between 1990 and 2017, emissions of nitrogen oxides (NO_x) from transport decreased by 40%, those of sulphur oxides (SO_x) decreased by 66 %, and those of both carbon monoxide (CO) and non-methane volatile organic compounds (NMVOCs) decreased by 87 %. Between 2000 and 2017, emissions of particulate matter with a diameter of 2.5 μm or less ($PM_{2.5}$) decreased by 44 % (Figure 1.7). [9]

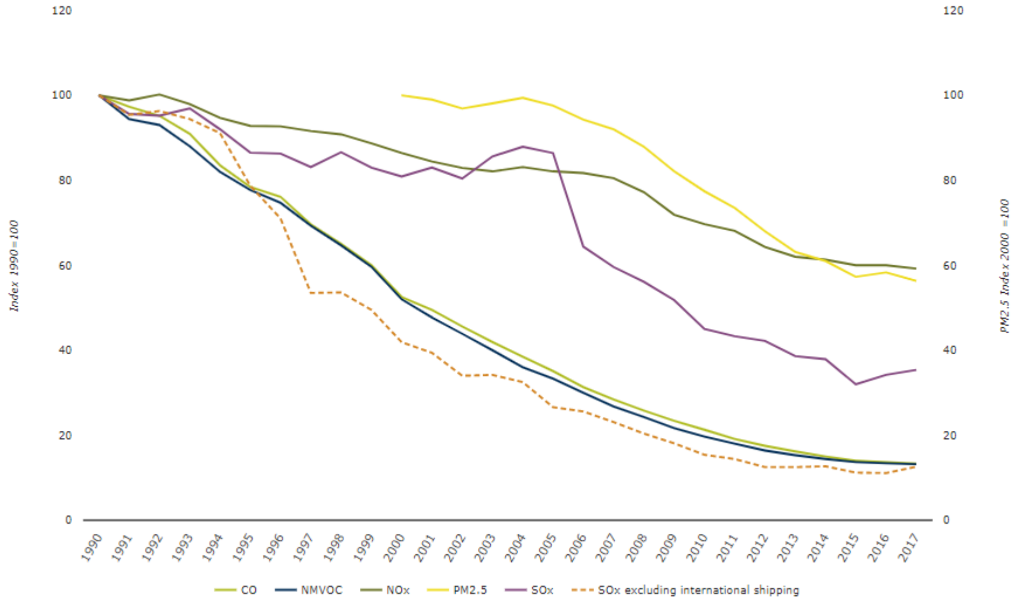

Figure 1.7 Trends in emissions of air pollutants from transport [9]

Despite these encouraging trends, transport remains responsible for more than two-thirds of all NO_x emissions and significantly contributes (around 10% of more) to total emissions of the other air pollutants. Road transport, in particular, continues to make a significant contribution to all the primary air pollutants (except SO_x). [9] The involvement of road transport to harmful NO_2 concentrations, especially in urban areas, is considerably higher because emissions occur close to the ground and mainly in densely populated areas.

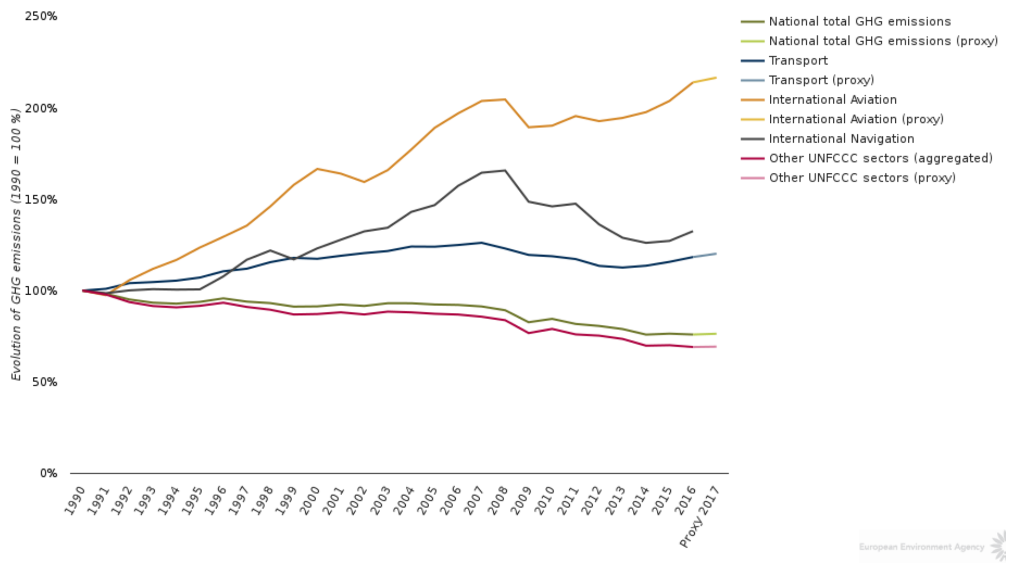

Figure 1.8 EU greenhouse gas emissions in the transport sector [10]

GHG emissions from transport (including international aviation but excluding maritime shipping) account for around one-quarter of the EU's total GHG emissions. CO_2 emissions from passenger cars, light commercial vehicles, and heavy-duty vehicles constitute by far the most considerable portion of transport GHG emissions.[11] Transportation is the primary European economic sector in which GHG emissions have increased (Figure 1.8). Preliminary data for 2018 show that they were 29% above 1990 levels. This increase is despite improvements in the efficiency of vehicles and is in line with increases in economic activity — measured by gross domestic product (GDP) — and increases in demand for passenger and freight transport [10].

1.2 Emission Legislations

1.2.1 Regulation on air pollutant emissions

To reduce the adverse effects on air quality caused by road transport emissions, EU emission standards for exhaust emissions have become increasingly stringent over the past decades. In this dissertation, the attention will be focused on the European regulation for Light Duty vehicles (i.e. passenger cars and light commercial vehicles). Since the 1970s, the key mechanism by which vehicle air pollutant emissions have been regulated has been through the setting of exhaust emission limits. As with CO_2 measurements, vehicle conformance with the required limits is checked based on standardised laboratory emission measurements. The first European Council Directive that specified measures against air pollution from motor vehicles was in 1970 (EU, 1970). Around 20 years later, in 1992, the 'Euro' emission standards were introduced, starting with the 'Euro 1' step, followed, generally, by successively stricter standards: Euro 2 to Euro 6. The evolution of Euro emission standards is summarised in Figure 1.9 [12].

Diesel	Date	CO	NMHC	NO_x	$HC + NO_x$	PM	PN
Euro 1	July 1992	2.72	–	–	0.97	0.14	–
Euro 2	January 1996	1.0	–	–	0.7	0.08	–
Euro 3	January 2000	0.64	–	0.50	0.56	0.05	–
Euro 4	January 2005	0.50	–	0.25	0.30	0.025	–
Euro 5a	September 2009	0.50	–	0.180	0.230	0.005	–
Euro 5b	September 2011	0.50	–	0.180	0.230	0.005	6.0×10^{11}
Euro 6	September 2014	0.50	–	0.080	0.170	0.005	6.0×10^{11}
Petrol	**Date**	**CO**	**NMHC**	**NO_x**	**$HC + NO_x$**	**PM**	**PN**
Euro 1	July 1992	2.72	–	–	0.97	–	–
Euro 2	January 1996	2.2	–	–	0.5	–	–
Euro 3	January 2000	2.3	–	0.15	–	–	–
Euro 4	January 2005	1.0	–	0.08	–	–	–
Euro 5	September 2009	1.0	0.068	0.060	–	0.005	–
Euro 6	September 2014	1.0	0.068	0.060	–	0.005	6.0×10^{11}

Figure 1.9 Emission limits (g/km) of the successively introduced Euro emission standards for passenger vehicles [12]

1.2.2 Regulation on GHG emissions

The CO_2 regulation for LDVs is one of the main pillars of the EU climate policy for transport. Binding CO_2 emission targets for newly sold vehicles have been set by Regulations (EC) 443/2009 for passenger cars (EC, 2009). The target set for passenger cars is 95 g/km to be met in 2021. This regulation should contribute to the overall GHG emission reduction goals of the EU, in particular, the 60% reduction of transport's GHG emissions in 2050 compared to 1990 and the 30% GHG emissions reduction for the non-ETS (non-Emission Trading System) sectors in 2030 relative to 2005. These targets are defined in terms of fleet-wide average Tank To Wheel (TTW) CO_2 emissions on the NEDC type approval test. These EU targets are applied to all transport modes except maritime. Electricity, biofuels and hydrogen count as zero-emission (IPCC definition) (EC, 2011a).

There are four main factors of influence on the target levels:

- the required emission reduction;
- the volume growth;
- the share of biofuels;
- the share of AFVs (and whether BEVs or PHEVs/REEVs are used).

Figure 1.10 summarises the required target levels to meet the 2050 and 2030 reduction goals, respectively. As shown, the target levels for the mid scenarios are stricter for meeting the 2030 goals compared to meeting 2050 goals. The bandwidth for 2025 ranges from 0 to 95 g/km, with mean values of 65 and 70 g/km. The bandwidth for 2030 ranges from 0 to 95 g/km as well, with mean values of 44 and 55 g/km.

	Target levels of new passenger cars in g/km	
	Mid value 2025 (bandwidth in between brackets)	Mid value 2030 (bandwidth in between brackets)
Target levels required to meet 2050 goal	**70** (43* to 84 g/km)	**55** (0 to 72 g/km)
Target levels required to meet 2030 goal	**65** (0 to 95 g/km)	**44** (0 to 95 g/km)

* Assuming that all AFVs are zero-emissions; in case these are (partly) PHEVs, the lower end of the bandwidth will be lower, up to 0 g/km).

Figure 1.10 Summary of target levels for cars for 2025 and 2030 [13]

Most scenarios require ZEVs and cannot be met with PHEVs alone (except for the designs with the least stringent reduction goals and with biofuels). [13]

The gap between official type approval and real-world CO_2 emissions results for new passenger cars increased from about 9% in 2001 to 42% in 2015 (Figure 1.11). The trend was particularly pronounced in recent years, with the gap more than doubling between 2009 and 2015. As a result, less than half of the on-paper reductions in CO_2 emissions since 2001 have been realised in practice. Since 2010, hardly any real-world reductions in CO_2 emissions have been achieved. The main reason for the widening gap is increasingly unrealistic type-approval CO_2 values that are generated as vehicle manufacturers more and more exploit loopholes in the NEDC testing procedure.[11]

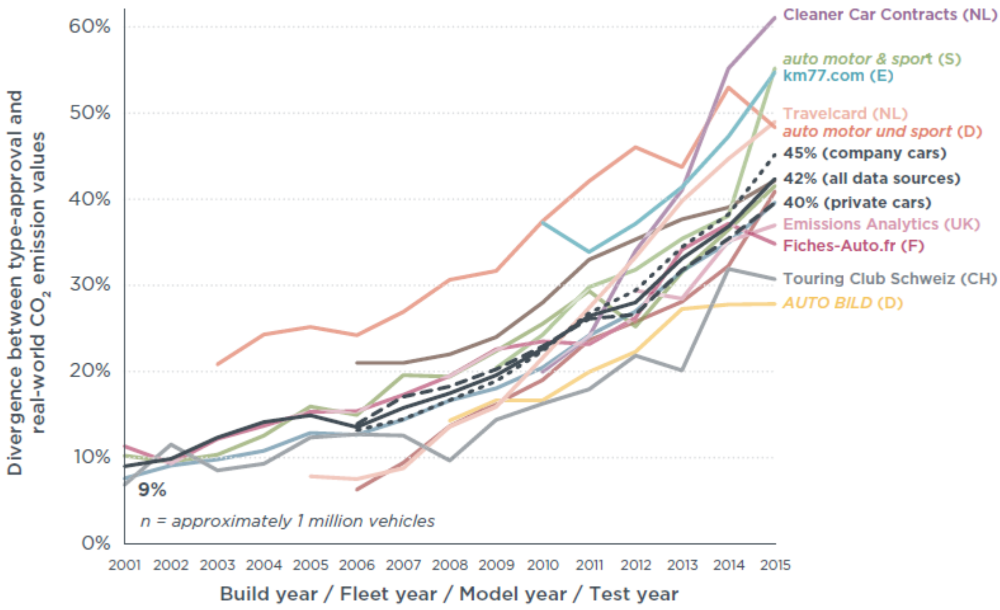

Figure 1.11 Divergence between real-world and manufacturers' type-approval CO2 emission values for various on-road data sources, including average estimates for private cars, company cars, and all data sources [11]

As a first step for reducing the gap between official and real-world CO_2 emission levels, a new vehicle-emissions testing procedure will be introduced, the Worldwide harmonised Light vehicles Test Procedure (WLTP), described in the Section 1.3.2[11].

1.3 Driving Cycles

According to Europe's legislation, before being sold, vehicles must be tested to verify they are compliant with the required environmental, climate, safety and security standards.

1.3.1 NEDC

In Europe the New European Driving Cycle (NEDC) chassis dynamometer procedure was used until September 2017. The NEDC was initially developed when vehicles were lighter and less performant than those available today. Nowadays the NEDC is outdated, with much evidence available from the scientific community and vehicle users clearly showing that the emission values and fuel consumption measured in the laboratory vastly underestimate the actual levels obtained under real-world driving conditions. The lack of correlation with the Real-World operating conditions can be attributed to [14]:

1. Real-world driving, which is more dynamic than the NEDC (i.e. show higher vehicle accelerations/decelerations due to more aggressive drivers' behaviours and different traffic conditions, as shown in Figure 1.12);
2. Real-world vehicle mass which is generally higher than type-approval;
3. Road incline;
4. Environmental conditions.

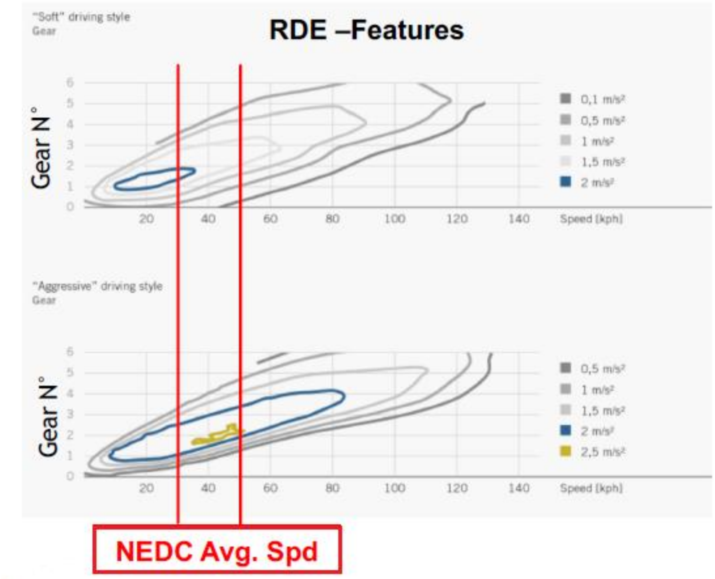

Figure 1.12 Real Driving Emission features [14]

1.3.2 WLTC

Since September 2017, the World Harmonised Light Vehicle Test Procedure (WLTP) has been introduced as the emission testing procedure for all new vehicle types replacing in Europe (NEDC) test procedure. It has become mandatory for all new passenger cars since September 2018 and for all new vans from September 2019. The road category (urban, rural, motorway) could not be used to have a worldwide harmonized test protocol due to differences in definitions and speed limits of these road categories from different regions. Therefore, it became necessary to develop the WLTC cycle on speed classes (low, medium and high speed) rather than on-road types (urban, rural, motorway) [15].

The new test includes a greater range of driving situations, more dynamic and representative accelerations and decelerations, more realistic driving behaviour, more realistic vehicle test mass, and stricter test conditions that better represent real-world driving conditions[12]. Figure 1.13 shows the speed profiles of WLTC driving cycle for Class 1, Class 2 and Class 3-2, the last one is appropriate for the power to mass ratio of the majority of European cars and it is the one used in this thesis work. The Class 3-2 is compared to the NEDC driving cycle in Figure 1.13.

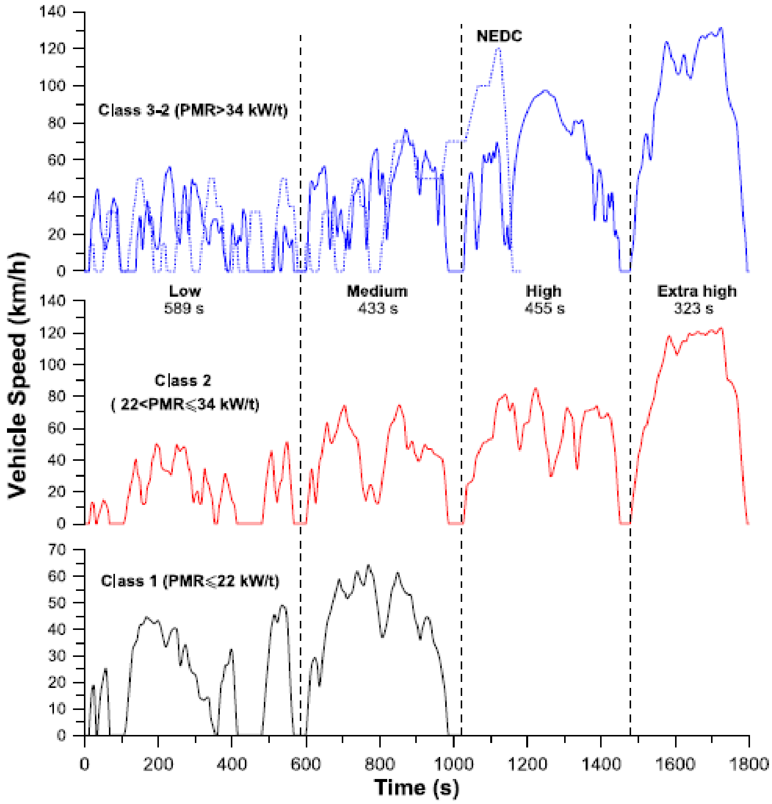

Figure 1.13 Speed profile of the WLTC driving cycles for Classes 1,2 and 3-2; discontinuous line along the Class 3-2 graph shows the Europe NEDC speed/time trace (PMR: power mass ratio) [16]

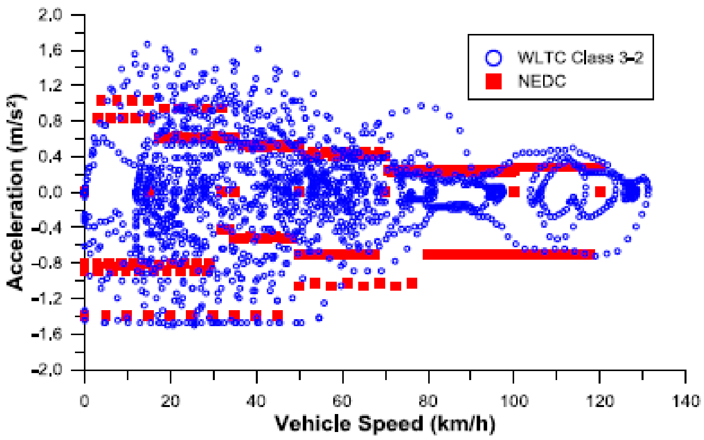

Figure 1.14 Comparison of the speed/acceleration distribution between the WLTC Class 3-2 and the NEDC [16]

Specification	NEDC	WLTC 3-2	Difference (from NEDC Values)	Effect
Duration (s) Distance (m)	1180 11,000	1800 23,266	+53% +112%	Lower influence of cold-start emissions
Average speed (km/h)	33.6	46.5	+38%	Most probably, better fuel efficiency
Maximum speed (km/h)	120	131.3	+9%	More realistic of today's driving habits
Idling time (%)	23.7	12.6	−47%	Lower influence of start-stop systems
Cruising (%) Transient time (%) Maximum acceleration (m/s^2) Average acceleration (m/s^2) RPA (m/s^2)	39.6 36.7 1.04 0.594 0.116	3.7 83.7 1.67 0.406 0.159	−91% +128% +60.5% −31% +37%	More transient, hence higher, pollutant and CO_2 emissions

Figure 1.15 Comparison of the technical specifications between the WLTC and the NEDC driving schedules [16]

The NEDC is quite simple to drive and thus easily repeatable. However, as already argued, it does not account for real driving behaviour in actual traffic, containing many constant-speed (Figure 1.13) and constant-acceleration segments (Figure 1.14). In fact, in Europe, the gap between fuel consumption and emissions experienced by the vehicle on the road and those measured at type approval is higher compared to other areas of the world [16]. Moreover, since it is only run once, cold started, its short distance might over-emphasize cold-starting emission effects (Figure 1.15).

The WLTC, compared to the NEDC, lasts longer, covers more than double distance, is characterized by fewer stops, less driving at a constant speed and more acceleration and braking (see Figure 1.15 that compares some important technical attributes of the two cycles). These differences are reflected in cold-start emission effects being relatively lower than NEDC ones. From a pure measurement/experimental point of view, the longer duration of the WLTC poses a burden on the test-bed capacity. Furthermore, the WLTC has both higher maximum and average driving speeds, and almost half the idling period.[16]

As Figure 1.16 illustrates, the gap between the *real-world* CO_2 emissions and the *official* ones is decreased considerably, moving on to WLTC procedure. However, it is estimated that this discrepancy will augment in the next years, and this led to the adoption of the Real Driving Emission test performed on the road.

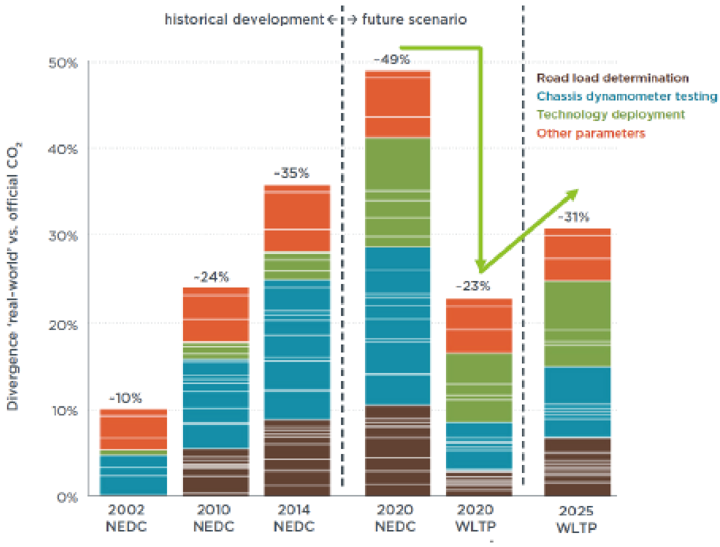

Figure 1.16 Divergence 'real-world' vs official CO_2 [14]

1.3.3 RDE

To help address the gap between legislative and real-world emissions, the European Union has recently agreed a Real Driving Emission (RDE) test procedure for cars and vans. The RDE is a test performed on the road. The new RDE procedure will measure emissions of NO_x, and at a later stage particles number, using Portable Emission Measuring Systems (PEMS) attached to the car. The RDE is composed of three segments (Urban, Rural and Motorway). Even though the RDE test is conducted on public roads open to traffic, there are provisions to ensure that test trips cover a broad range of driving conditions typically encountered by European drivers. Figure 1.17 shows the set boundaries that define what constitutes an RDE trip valid. The laboratory NEDC test represents a fixed set of testing conditions, such as a predetermined speed profile and a narrow ambient temperature range of 20°C to 30°C, so that the test is repeatable and reproducible. By contrast, the RDE test has a broader range of parameters, each with ample margins allowed to cover a broad spectrum of driving possibilities. For ambient conditions of temperature and altitude, two sets of boundary conditions exist "moderate" and "extended". If a data point falls within the extended conditions, the emissions measured have to be divided by a factor of 1.6. Any data point falling outside of the boundary conditions makes the whole trip invalid [17].

Parameter		Provision set in the legal text
Payload		≤90% of maximum vehicle weight
Altitude	Moderate	0 to 700 m
	Extended	Between 700 and 1300 m
Altitude difference		No more than a 100-m-altitude difference between start and finish
Cumulative altitude gain		1200 m/100 km
Ambient temperature[14]	Moderate	0°C to 30°C
	Extended	From -7°C to 0°C and 30°C to 35°C
Stop percentage		Between 6% and 30% of urban time
Maximum speed[15]		145 km/h (160 km/h for 3% of motorway driving time)
Dynamic boundary conditions	Maximum metric	95th percentile of *v*a* (speed * positive acceleration)
	Minimum metric	RPA (relative positive acceleration)
	Curves shapes shown in Figure 2.	
Use of auxiliary systems		Free to use as in real life (operation not recorded)

Figure 1.17 Boundary conditions for RDE tests [17]

The new protocol requires the real driving emissions from cars and vans to be lower than the legal limits multiplied by a 'conformity factor'. This factor expresses the ratio of on-road PEMS emissions to the legal limits [12].

2 Hybrid Electric Vehicles

2.1 Hybrid Electric Vehicles

Hybrid Vehicles combine two or more sources of power that can directly or indirectly provide propulsion. The basic idea is to have high-specific energy coupled with a reversible one, for storing energy coming from regenerative braking. [7] Although with this definition, many configurations of hybrid vehicles are possible, only Hybrid Electric Vehicles (HEVs) have effectively reached the mass market. [4]

HEVs use electrochemical batteries as the RESS, and electric machines (one or more) as secondary energy converters, while a reciprocating internal combustion engine (ICE), powered by a hydrocarbon fuel, serves as the primary energy converter. The electrochemical battery can be used for regenerative braking and also acts as an energy buffer for the thermal engine, which can instantaneously deliver an amount of power different than what is required by the vehicle load, employing one or more electric machine. The EMs can work as generators, recovering the kinetic energy during the brake and converting it into electricity to be stored in the battery.

This engine management flexibility allows keeping the engine more often operating in its high efficient or less polluting region. Other benefits offered by hybridization are the possibility to shut down the engine when it is not needed (such as at a stop or low speed), and the downsizing of the engine: since the peak power can be reached by summing the output from the engine and the RESS, the former can be downsized, i.e. replaced with a smaller and less powerful engine, operating at higher average efficiency. [18]
In the literature, different ways of classifying the HEVs have been proposed. Some of them have been reported in this treatise.

2.1.1 Hybridization levels

In order to cover automotive needs, various hybrid electric vehicle concepts have been proposed and developed. According to the size of the electric machine size and the enabled functionalities, Figure 2.1 shows a possible classification of today's vehicles in the market [18][19].

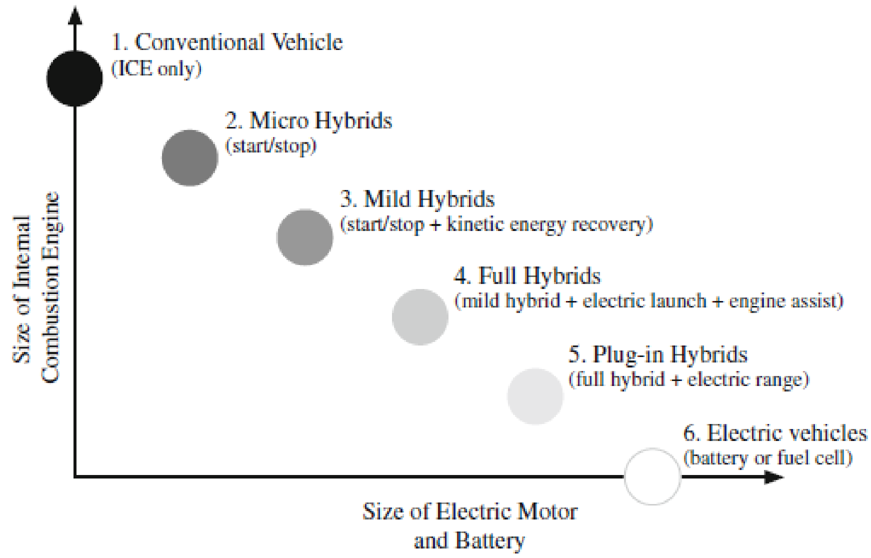

Figure 2.1 The spectrum of vehicle hybridization levels[18]

- **Micro hybrid** means generally nonelectric vehicles that feature start-stop systems; fuel economy can be improved by 5-10% during city driving condition.
- **Mild hybrid** electric vehicles typically have the ICE couples with an electric machine; the electric motor assists the internal combustion engine during aggressive acceleration phases and enable to recover most of the regenerative energy during deceleration phases. Mild hybrid electric vehicles do not have an exclusive electric-only propulsion mode. The fuel economy improvement is mainly achieved through shutting down the engine when the car stops, using electrical power to initially start the vehicle, optimizing engine operational points, and minimizing engine transients. Typical fuel savings in vehicles using mild hybrid drive systems are in the range of 15 to 20%.
- **Full hybrid** electric vehicles run on just the engine, only the battery, or a combination of both. Compared with traditional internal combustion engine vehicles, the overall fuel economy of a full hybrid electric vehicle in city driving could improve by up to 40%.
- **Plug-in hybrid** electric vehicles (PHEVs) share the characteristics of both full hybrid electric vehicles and all-electric vehicles with the capability of charging the battery through an AC outlet connected to the electric grid.
- **Electric vehicles** are propelled only by their onboard electric motor(s), which are powered by a battery (recharged from the power grid) or a hydrogen fuel cell.

Table 2.1 summarises the main described characteristic of various hybrid electric vehicles.

Type of vehicle	Features and capabilities				
	Start–stop	Regenerative braking	Boost	Electric-only mode	Electric range (miles)
Micro hybrid	Yes	Possible	No	No	No
Mild hybrid	Yes	Yes	Yes	No	No
Full hybrid	Yes	Yes	Yes	Possible	Possible (<2)
Plug-in hybrid	Yes	Yes	Yes	Yes	Yes (20–60)
Pure electric	Yes	Yes	Yes	Yes	Yes (80–150)

Table 2.1 The main features and capabilities of various hybrid electric vehicles [19]

2.1.2 Hybrid Architectures

Hybrid Electric Vehicles can be distinguished in *simple architecture* and *complex architecture*.

The **simple hybrid architecture** is obtained combining two traction systems, one topology for each category of power actuator: one internal combustion engine and one electric motor. Depending on the choice of the connection between the two tractions system, it is possible to distinguish: *Series Architecture* and *Parallel Architecture*.

- **Series Architecture**

In the series architecture, the only power actuator connected to the wheel is an electric motor (Figure 2.2). The internal combustion engine is mechanically disconnected from the wheel, and it is used as an Auxiliary Power Unit (APU); it is connected to a generator used to produce electricity that can either be stored in the battery or directly sent to the EM. An electrical link connects the traction system.

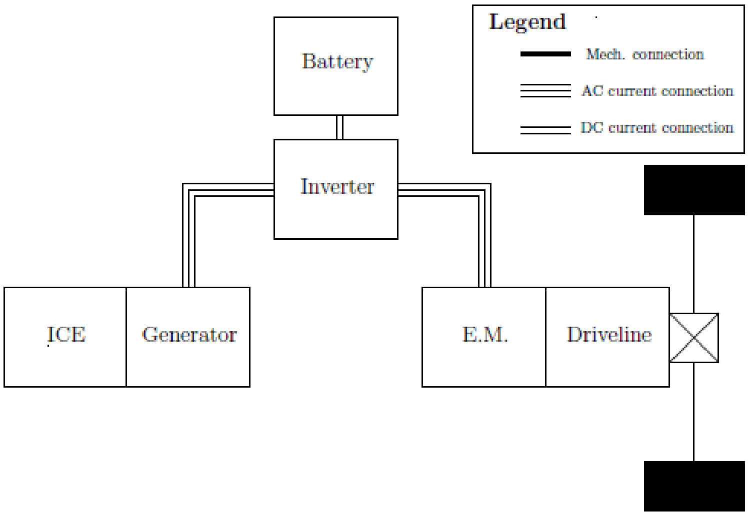

Figure 2.2 Scheme of a series hybrid architecture

Since the engine is decoupled from the wheel, it can operate quite close to its maximum efficiency region, and it is possible to strongly simplify the transmission thanks to the shape of the torque curve of the EM. The disadvantage of architecture, represented by Figure 2.2, is the significant inefficiencies related to multiple conversions of mechanical energy into electrical energy and vice versa.

A parameter, named Hybridization Ratio, is used to assess the share of power between the battery and the auxiliary power unit. In the case of series configuration, its definition is shown in the Eq. 1:

$$R_{h\ Series} = \frac{P_{EL\ GEN}}{P_{EM}} \qquad \textit{Eq. 1}$$

Where $P_{EL\ GEN}$ is the power of electric generator and P_{EM} is the power of the electric machine. The series hybridization ratio ranges from 0 (pure Battery Electric Vehicle) to 1 (Electric Transmission) as shown in Figure 2.3:

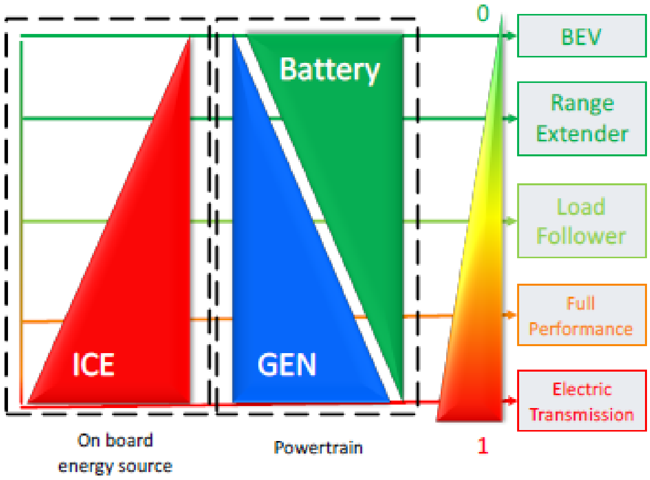

Figure 2.3 Series Hybridization Level [20]

The value of 0 series hybridization ratio means no generators, installed so a BEV with no additional energy sources. As the size of the generator increase, the size of the battery decreases reaching at first the range extender configuration that is characterised by very small ICE (APU) (that works only in the case of high-power request and when the battery is fully discharged in order to enable the last mile distance between the recharge), the battery produces most of the power. In the load follower and full performance configurations, the propulsion for moving the vehicles could be provided in higher share by the APU instead of the battery. When ($R_{h\,Series} = 1$) electric transmission is realised, with no battery, and the ICE provides all the power.

- **Parallel Architecture**

Differently from the series architecture, the link between the ICE and the EMs is mainly performed at the transmission level through a mechanical connection. Both actuators can provide the power to the wheel, and this gives the possibility to sum the power of the two machines and to avoid the multiple efficiency drops, typical of series architecture. However, unless significantly oversized, the electric motors are less potent than those used in a series hybrid (because not all the mechanical power flows through them), thus reducing the potential for regenerative braking. Moreover, the engine operating conditions cannot be freely determined as in a series hybrid architecture, because its speed is mechanically related (via the transmission) to the vehicle velocity. Another disadvantage is the need to have a transmission with a multi-gear configuration [18].

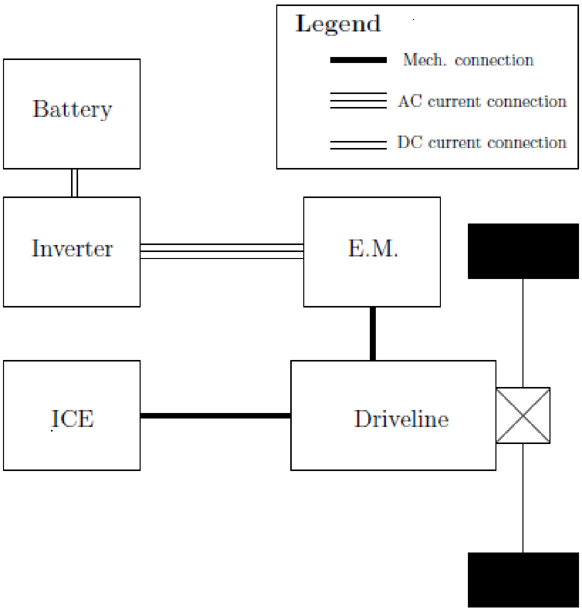

Figure 2.4 Scheme of a parallel hybrid architecture

As for series architecture, it is possible to define the Parallel Hybridization Ratio with the Eq. 2:

$$R_{h\ Parallel} = \frac{P_{EM}}{P_{ICE} + P_{EM}} \quad \textit{Eq. 2}$$

Whereas in the series configuration the ICE is an auxiliary power generator, in the parallel one it represents one of the two actuators. The following figure depicts the possible hybridization levels of a parallel configuration.

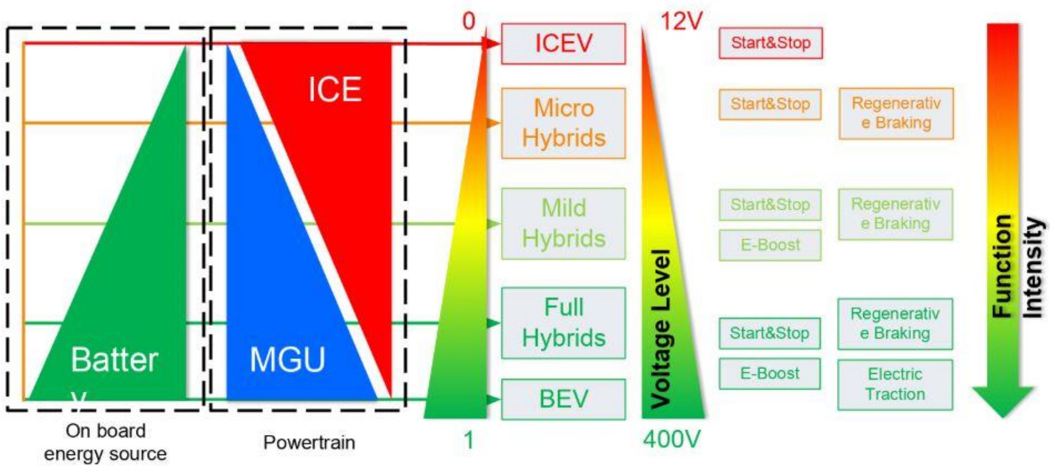

Figure 2.5 Parallel Hybridization Level [20]

As illustrated in Figure 2.5, the hybridization ratio lower, the power of ICE when $R_{h\ Parallel} = 1$ until only the battery and the electric motor are present in the BEV.

Differently from the series configuration, a change of hybridization ratio implies a variation of the functionalities.

A possible classification of parallel hybrid architecture is according to the EMs position (Figure 2.6). In such a framework, it is worth to describe only the general character of the primary configurations.

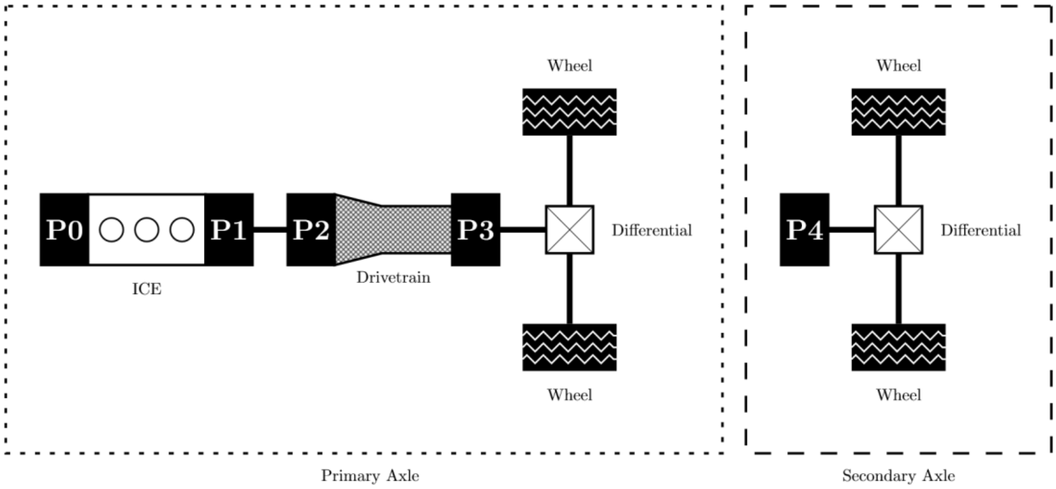

Figure 2.6 Classification of parallel hybrid according to the EMs position [20]

- **P0**

The EM is always mechanically connected, usually belt-connected, to the engine. The regenerative braking potentialities are limited, and the purely electric mode is not attainable. An example of P0 hybrid vehicle is the Renault Scenic Hybrid Assist composed of 48V battery system and low-cost components [21].

- **P1**

Between the EM and ICE, there is a mechanical connection without the possibility of disconnection between the engine itself. Mercedes s400 Hybrid is an example of P1 hybrid electric vehicle; an active flywheel, a 48 V system and medium-cost component constitute it [22].

- **P2**

It is one of the most used configurations. The EM is placed between the transmission and ICE, on the transmission side. It is possible to disconnect the EM from the ICE through a clutch avoiding the dragging of the ICE with the EM during the pure-electric drive. Sample of this configuration is the Hyundai Ioniq [23].

- **P3**

The EM is positioned downstream of the gearbox, it is integrated with the transmission shaft, and its speed is a multiple of the wheel speed. The connection is obtained through a gear mesh. The Ferrari LaFerrari is a P3 hybrid electric vehicles composed of high voltage system and high-cost component, as the previous example, with an increase transmission volume [20].

- **P4**

The EM is located on the opposite axel than the ICE, and the connection is through a gear mesh or simple transmission. This configuration allows the electric-all-wheel drive. Porsche 919 Hybrid is a P4 HEV model with high voltage system and high-cost components [20].

It is possible to obtain **complex hybrid architectures** in different ways:

- increasing the number of traction motors or ICEs;
- increasing the amount of energy and power sources;
- coexistence in the same architecture of a parallel path with a series one.

In such a framework, it is worth to mention two particular cases which are quite relevant among complex hybrid architectures.

- **Series/Parallel architecture**: this drivetrain combines the advantages and disadvantages of the parallel and series drivetrains. By combining the two designs, usually, through one or more clutches, the engine can both drive the wheels directly (as in the parallel drivetrain) and be effectively disconnected from the wheels so that only the electric motor powers the wheels (as in the series drivetrain). A representative model is the Koeninggseg Regera (Figure 2.7).

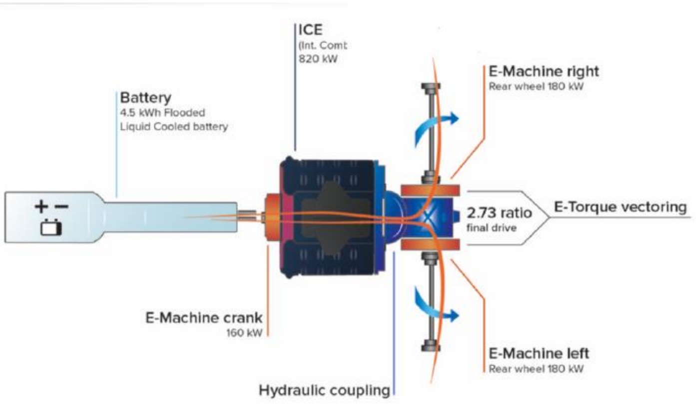

Figure 2.7 Koeninggseg Regera architecture

- **Power split architecture**: this is a complex hybrid in which the power is always divided between a parallel and series path. The combination of the operating mode is based on a planetary gear set where the generator is connected to the sun gear, the engine to the planetary carrier and the electric motor to the ring. The significant part of hybrids belonging to this category are produced by Toyota, and they are based on the THS (Toyota Hybrid System) of the Toyota Prius [7].

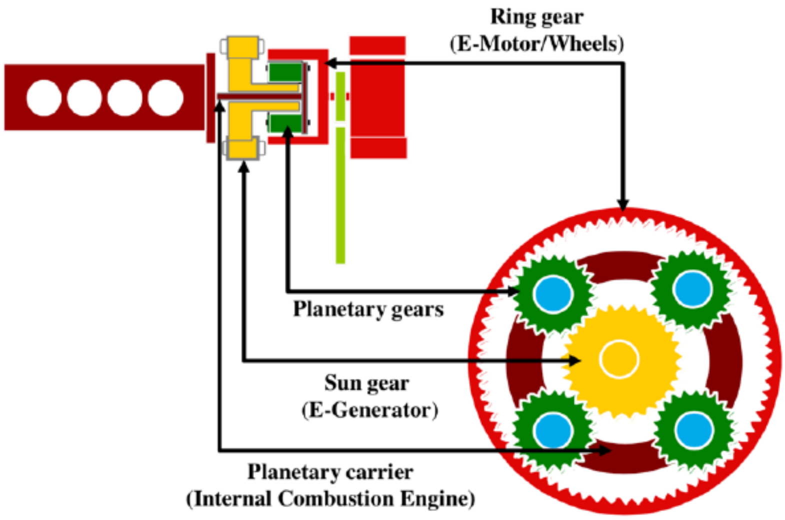

Figure 2.8 Toyota Hybrid System architecture

3 Control Strategies for Hybrid Vehicles

3.1 Energy Management in HEVs

Hybrid powertrains, independently from the arrangement, possesses several sources and several power actuators. This additional degree of freedom provides some challenges in controlling how much power should be supplied from each power actuator installed. These challenges are overcome by adding a layer of control, the so-called high-level control, to the conventional low-level one: Energy Management System (EMS).

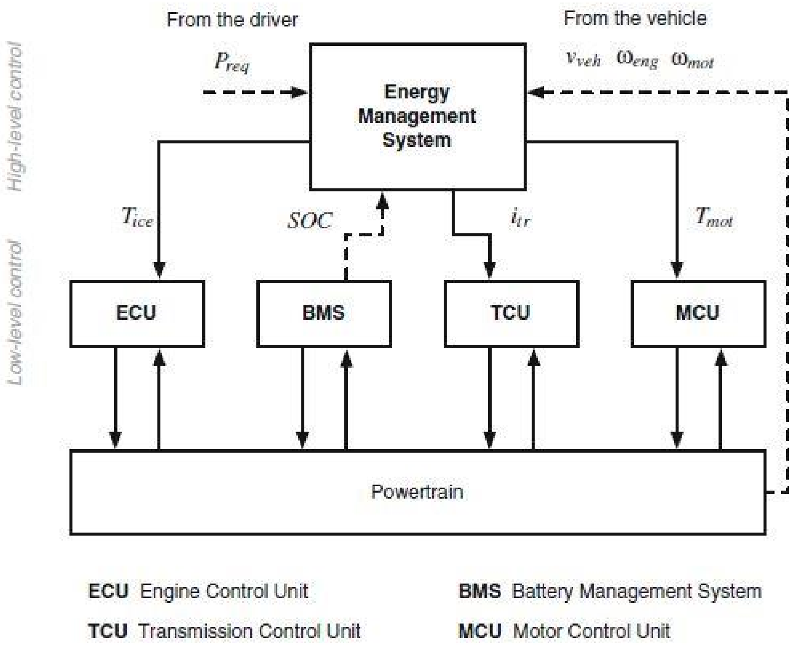

Figure 3.1 Two-layer architecture in a hybrid vehicle [18]

This layer of control receives the state of the car, and the driver demands to output the set-points that will be sent to the low-level control layer that in turn control each powertrain component by using classical feedback control methods [18].

The Energy Management System could be further divided into two different subsystems:

1) **Supervisory controller**: which decides the best operating mode (ICE only, parallel, EV etc.) based on the driver demand and the working conditions of the components;
2) **Energy Management Strategy**: once the Supervisory has decided the mode, it splits the power among ICE and EMs to satisfy the overall power demand

There are various approaches to evaluate optimal control laws.

3.2 Problem Formulation

The function of the energy management strategy in HEVs is to define the best power split capable of achieving the target of the vehicle. This target could concern performance, including emissions, fuel economy and other possible costs by splitting the power demand between the engine and the battery. In general, it is possible to define the objective of hybridization as the minimization of a given cost function (or performance index), e.g. representing the fuel consumption as shown in Eq. 3:

$$J = m_f(T) = \int_0^T \dot{m}_f\left(t, u(t)\right)dt \qquad \textit{Eq. 3}$$

Where J is the cost-to-go function to minimize, $m_f(T)$ is the cumulative fuel consumption over the mission profile, $\dot{m}_f\left(t, u(t)\right)$ is the instantaneous fuel consumption, $u(t)$ is the vector of control variables that leads to the minimization of the fuel consumed, and T is the duration of the vehicle mission. The minimization of J is subjected to constraints such as physical limitations of the actuator, restrictions in the energy stored in the RESS and the requirement to maintain the battery SOC within prescribed limits. These limits make the design of the energy management a constrained, finite-time optimal control problem characterized by a set of both local and global constraints, on the state and control variables, that minimize the objective function [18].

3.3 Control strategies

There are three main objectives which are requested from every hybrid vehicle: low fuel consumption, acceptable performance and drivability. First one is satisfied by optimal control strategy and the two latter ones by shifting strategy, SOC control and ZEV (Zero Emission Vehicle) operation of the vehicle. Not all three objectives can be entirely satisfied at the same time, and there must be a trade-off between them. [24]

The control law strategies [25] can be grouped into three categories:

1) **Global Optimization strategies**, in which the dynamic nature of the system is considered for optimization. These strategies are characterized by the highest computational time and can only be used for benchmarking. The most common example of such strategies is Dynamic Programming.
2) **Static optimization strategies**: they are instantaneous optimization; they consist of an instantaneous minimization of a cost function, taking into account both the engine fuel consumption and the use of the electrical energy stored into the battery. They have no information about the future. These strategies are less effective than the Global Optimization ones, but they need less computational efforts. A representative example of this category is the Equivalent Consumption Minimization Strategy.
3) **Heuristic strategies** (also known as rule-based): they are based on simple laws that are defined based on some operating control of the vehicle and usually aim to help the engine to operate at low emission and/or high-efficiency regions. These are the most common strategies since thanks to their low computational requirements, and they can be easily implemented in an ECU.

It is crucial to identify the so-called **feasible strategies**: a strategy that can be implemented at real-time in a real ECU considering the single-vehicle perspective, neglecting any communication with external devices. Examples of possible feasible approaches are:

- Equivalent Consumption Minimization Strategy
- Model Predictive Control
- Rule-based control

Not-feasible strategies are:

- Dynamic Programming
- Pontryagin’s minimum principle

These last two strategies require high computational power, and they need knowledge of the future. Nevertheless, this kind of strategies can be used to benchmark solution (global optimum) and then can be used to develop rule-based strategies. Knowing what the optimal solution is, is crucial to improve the design and to minimize costs.

3.4 Dynamic Programming

3.4.1 General concepts

The dynamic programming is a numerical method that finds the optimal global solution of multistage decision-making problems by operating backwards in time.

Dynamic Programming is based on Bellman's principle of optimality:

An optimal policy has the property that whatever the initial state and initial decision are, the remaining decisions must constitute an optimal policy with regard to the state resulting from the first decision.

This means that from any point on an optimal trajectory, the remaining trajectory is optimal for the corresponding problem initiated at that point.

Since DP is commonly used to solve time-continuous control problems, the model has to be discretised in a sequence of time steps for which DP is capable of determining the optimal control laws. The optimal cost-to-go function is then computed for each value of the state variables x (for instance the State Of Charge of the battery) in the acceptable range following a backward path starting from the final time and state [7].

From the mathematical point of view, consider the discrete-time system $x_{k+1} \in \Omega_k$:

$$x_{k+1} = f_k(x_k, u_k) \qquad \textit{Eq. 4}$$

Where k=0,1…,N-1 represents the time steps, x_{k+1} the state variable at time step $k+1$ and $u_k \in U_k$ that is the control variable at time k.

The control policy is:

$$u = \{u_0, u_1, \dots, u_{N-1}\} \qquad \textit{Eq. 5}$$

The cost of the policy, starting at the initial condition x_0, is

$$J(x_o, u) = L_N(x_N) + \sum_{k=1}^{N-1} L_k(x_k, u_k) \qquad \textit{Eq. 6}$$

Where L_k is the instantaneous cost function, also called arc cost. The optimal cost function is the one that minimises the total cost:

$$J^*(x_0) = \min_u J(x_0, u) \qquad \textit{Eq. 7}$$

The corresponding optimal policy is: $u^* = \{u_1^*, u_2^*, \dots, u_{N-1}^*\}$:

$$J_{u^*}(x_0) = J^*(x_0) \qquad \textit{Eq. 8}$$

Considering now the "tail subproblem" of minimising the cost-to-go Y from i (and state x_i) to time N:

$$Y(x, i) = L_N(x_N) + \sum_{k=1}^{N-1} L_k(x_k, u_k) \qquad \textit{Eq. 9}$$

Bellman's principle states that the "tail policy" $\{u_i^*, u_{i+1}^*, \dots, u_{N-1}^*\}$ is the optimal policy for the tail subproblem. This statement finds an analytical justification in the induction principle.

Therefore, the algorithm proceeds backwards, starting from the final step N it is determined the optimal sequence of control actions choosing at each step the path that minimised the cost-to-go (integral cost from that time step until the final state). The optimal cost-to-go can be mathematically expressed in the Eq. 10: [18]

$$u_k = \mu^*(x_k, k) = \arg\min_{u \in U_k} \left(L_k(x_k, u) + Y_{k+1}(f_k(x_k, u_k), u_k) \right) \qquad \textit{Eq. 10}$$

For k=N-1,N-2,…,1.
$Y(x_1, 1)$ generated at the last iteration is equal to the optimal cost $J^*(x_0)$.[4]

The dynamic programming algorithm provides the optimal solution to the HEV energy management problem and serves as a benchmark to assess the minimum fuel economy achievable along with a driving mission [26]. The sequence of controls u_k represents the power split between the ICE and the rechargeable energy storage system at successive time steps. The cost corresponds to fuel consumption, energy consumption, emissions, or any other design objective. The set of choices at each instant is determined by considering the state of each powertrain component and the total power request. Given the current vehicles speed and the driver's demand, the controller determines the full power that should be delivered to the wheels.

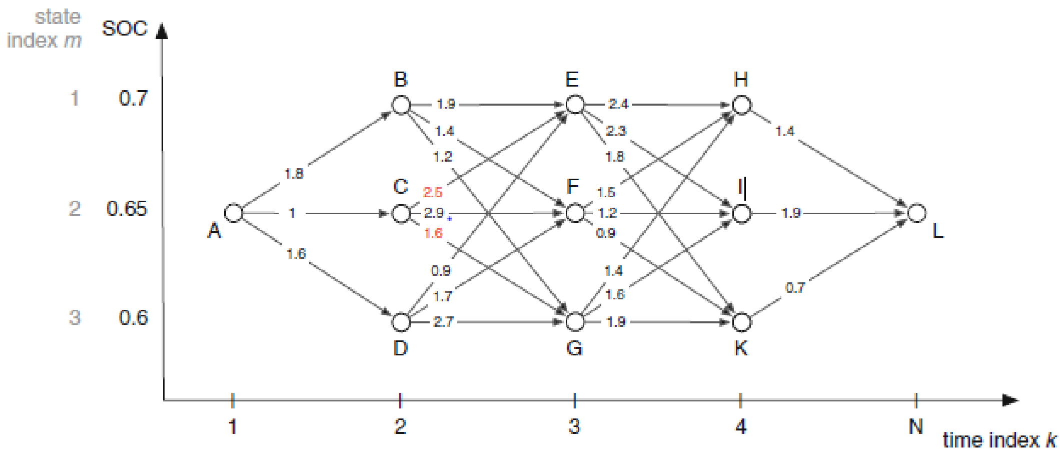

Figure 3.2 Arc costs in the simplified example

The procedure can be explained with the example shown in Figure 3.2, which refers to a generic HEV configuration with a single degree of freedom.

In this formulation, the stage variable is the time and the state variable x, represented by the points of the grid, is the State of Energy (SOE) of the battery. The arc cost is represented by the cost function (performance index). The maximum and the minimum slope of each operation is defined by the limits of constraints on the state variable, in this case, are the limits on the power actuator, corresponding the minimum and maximum power that the electric motor can absorb. The restrictions on the power actuator are in terms of maximum and minimum variation of SOE between two subsequent time steps. The procedure of DP starts from calculating all the arc costs, the costs of moving from all admissible nodes at time k to all the admissible nodes at time k+1. The second step consists in calculating the cost-to-go, starting from the final point and going backwards. The cost-to-go of each step is the minimum cost associated with moving from one node to another.

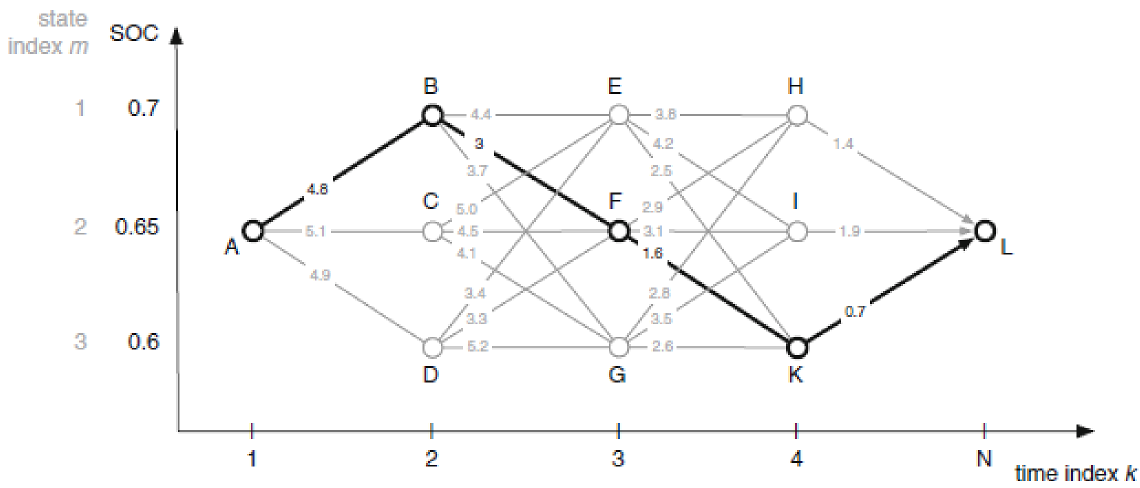

Figure 3.3 Cost-to-go and optimal path in the simplified example

DP provides a numerical optimal solution, within the accuracy limits due to the discretization of the candidate solutions. However, it is not applicable in real-time for two reasons:

1) the solution has to be calculated backwards; therefore the entire driving cycle must be known a priori, and
2) it is a procedure computationally heavy, requiring the backward solution of the whole problem before being able to determine the first control action.

However, dynamic programming provides the closest approximation to the optimal solution of the energy management problem. It is often used to determine the maximum potentiality of a given architecture, thus serving as a design tool or as a benchmark for implementable control strategies [7].

4 Modelling Approach

4.1 Introduction

As explained in Chapter 1, the automotive sectors in moving towards the electrification of the vehicles and the Hybrid Electric Vehicle represents the best choice for the near future, since it combines the high range of the thermal machine and the low pollutant emissions of electric machine. Unfortunately, hybrid powertrain models are characterised by complex mechanical systems. On the other hand, OEMs are facing a significant increase in the number of tests which are needed to calibrate this new generation of electrified powertrains over a variety of different driving scenarios. This context led to the proposal of various vehicle simulation models in the recent last year. Since control logics and system, configurations are incredibly complex, and a wide range of different options has to be explored, designing and developing hybrid powertrains based on chassis dynamometer or real driving tests becomes complicated and limited. Therefore, the simulation approach becomes crucial for exploring the wide range of possible combinations between different powertrain architectures, control strategies and working conditions. It is necessary to enable a cost-effective Hardware-in-the-Loop (HiL) testing (test conducted once production controllers are available), to speed-up the workflow thanks to process automatization and to avoid a large number of experiments and measurements for product validation [27].

Since one of the main objectives of this analysis is to estimate the engine fuel consumption and pollutant emissions in different driving conditions, the next sections will provide a brief description of the three most common modelling approaches suitable for this application and the delineation of fundamental equations and numerical models for the primary powertrain subsystem.

4.2 Backward Kinematic Analysis

The kinematic approach is based on a backward methodology. The backward approach is usually adopted for predicting vehicles fuel economy or emissions during the driving cycle. This analysis is based on a non-causal model causal (since it requires the entire driving cycle to be known in advance), because the calculation process starts from a prescribed profile of velocity used to calculate the tractive force at the wheel, and works “backward” calculating the engine torque and the fuel consumption (Figure 4.2b). The driving cycle is divided into small time intervals where speed, torque, and acceleration remain constant.

The engine speed is determined from simple kinematic relationships, starting from the wheel revolution speed and the total driveline transmission ratio. In contrast, the traction force that should be provided to the wheels to drive the vehicle, according to the chosen speed profile, can be calculated from the main vehicle characteristics (i.e. vehicle mass, aerodynamic drag and rolling resistance). Once the engine Brake Mean Effective Pressure (BMEP), that is strictly correlated to the needed tractive force, and the speed have been determined, the following 0D black-box model of the engine can be used to find the instantaneous fuel consumption or emission rate, as shown in Figure 4.1.

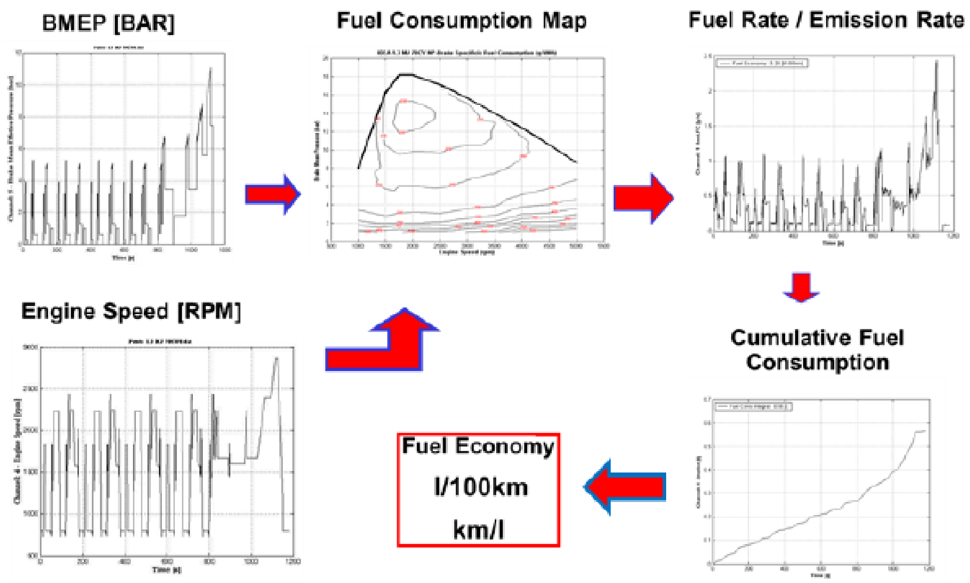

Figure 4.1 Information flow in a backward model for motor vehicles fuel consumption calculation

Obviously, this approach neglects all the dynamic phenomena considering transient conditions as a sequence of stationary states; therefore it is often used only for a first preliminary estimation of the fuel consumption or engine emissions of a motor vehicle, although the simulation results can differ significantly from the experimental data due to these simplifying assumptions. Furthermore, because of its backward approach, it assumes that the driving profile will be exactly followed, but, on the other hand, there are no guarantees that a given vehicle will be able to meet the desired speed trace. Despite its simplicity, such an approach has proved to be appropriate for the calculation of the instantaneous fuel consumption over the most common regulatory driving cycles, due to moderate speed and load transients that are usually prescribed (especially in the NEDC). [28][29]

4.3 Quasi-Static Analysis

In the quasi-static approach, as the forward dynamic process reported in Section 4.4, a driver model (typically a PID) compares the target vehicle speed with the actual one and generates a power demand profile to follow the target vehicle speed profile, by solving the longitudinal vehicle dynamics equations. Then, once the engine speed and the BMEP have been obtained, fuel consumption or pollutant emissions can then be calculated through interpolation of engine maps, as in the kinematic methodology which was described in the previous section. The simulation model can therefore be regarded as a "quasi-static" model, since, although system dynamics are taken into account, the behaviour of the primary devices (ICE, EM, batteries) is described through steady-state performance maps. [30] The quasi-static approach is suitable for evaluating the fuel consumption and NOx emissions of a vehicle performing the NEDC with reasonable accuracy (see [28] for more details). On the other hand, the same approach does not provide satisfactory results when used for different applications, as to predict soot emissions, since the acceleration transients and the related "turbo-lag" phenomena significantly contribute to the cumulative cycle emissions, thus requiring a more detailed engine simulation model, capable of also capturing the engine transient behaviour properly.

4.4 Forward Dynamic Analysis

Finally, in the fully dynamic approach, not only the longitudinal vehicle dynamics equation is solved to determine the engine speed and the torque demand, but also the internal combustion engine behaviour during transients is modelled using detailed OD or 1D fluid-dynamic models. For instance, for an internal combustion engine, the intake and exhaust systems can be represented as a network of ducts connected by junctions that represent either physical joints between the ducts, such as area changes or volumes, or subsystems such as the engine cylinder.

The forward modelling approach reproduces the physical causality of the system; the output is always an integral function of the input, inducing a time delay from the input to the output. Hence, forward modelling respects the physical limitations of the powertrain components. As shown in Figure 4.2a, the driving cycle generates the speed set-point that the driver needs to follow. The driver model can employ a Proportional-Integral-Derivative (PID) controller to compute the desired torque for the power actuators. The heart of the control layer is the energy management strategy block, which generates the reference control signals (e.g. the requested torque for ICE and EM). The actual speed, which is an integration of the tractive force generated by the powertrain, is then fed back to the driver and the

EMS blocks. The forward approach requires a longer computation time than the backward counterpart, owing to the inherent delay time of the causal principle. This disadvantage makes backward procedures more suitable for optimisation in terms of the computational cost.[31]

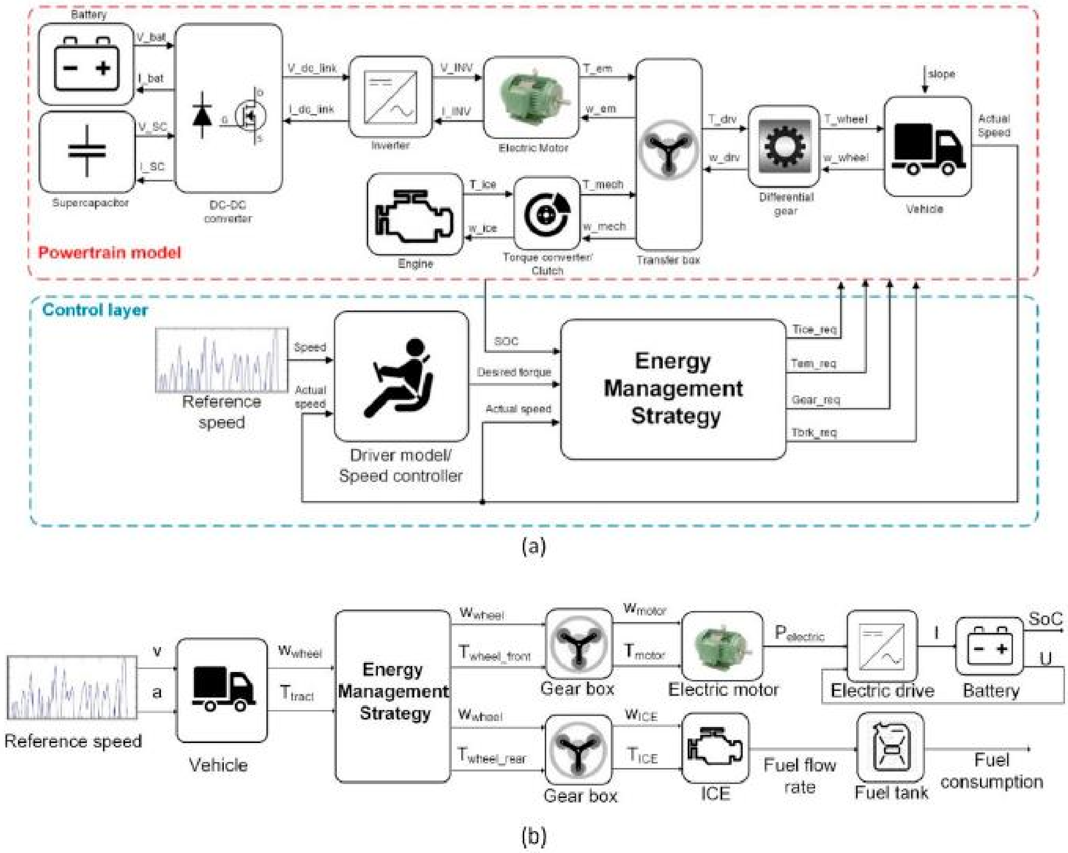

Figure 4.2 Modelling approach of a parallel HEV: (a) forward- and (b) backward-facing models

4.5 Powertrain modelling

To properly understand the operating principles of a Hybrid Electric Vehicle, it is very important to identify the main power actuator of the powertrain and to analyse the energy flow on the vehicle.

4.5.1 Engine

Depending on the timescale and the nature of the modelled system, different degree of detail can be adopted for the internal combustion engine modelling. In Figure 4.3, the main engine modelling methodologies are shown. The y-axis represents the time required for the simulation in terms of multiple of real phenomenon duration.

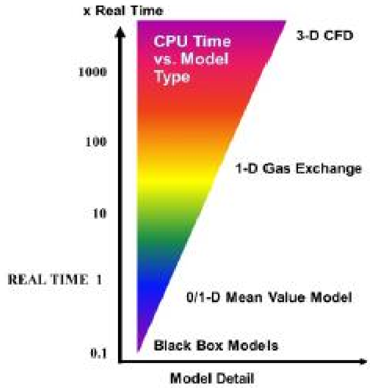

Figure 4.3 Main engine modelling methodologies [30]

3D CFD is the most complete and detailed methodology, and it can usually provide only component level detail but cannot usually provide a system-level perspective since, because the computational time increases with the system volume to be discretized, this approach is generally applied only to a specific engine component. 1D fluid dynamic simulation tools are usually used to provide a system-level perspective. 1D CFD allows having a good level of prediction both under steady-state operating conditions and during transient phases. And, if compared to real-time, the computational time required is not excessive. OD black-box models, also known as *map models*, are suitable for fuel consumption and emission calculations on type approval driving cycles, where transients are relatively smooth and can be simulated using a sequence of the stationary state. The ICE is modelled by means of experimental steady-state maps where the engine efficiency, power loss and fuel consumption are defined. The instantaneous fuel consumption and emissions rates are obtained by maps interpolation. The "mean value" model, instead, combine the low computational requirements of black-box models with the accuracy of 1D models. It reduces the 1D detailed model complexity while a physical description of the main phenomena is maintained [30].

The model used in this study is the *map model* since the analysis is focused on consumptions. The mechanical characteristics of the engine are represented by maps of the engine performance, at maximum load and minimum load, in terms of power and torque depending on the speed. The consumptions are calculated through a *Fuel Rate Map* in which the fuel consumption rate is in terms of engine speed and load.

It is worth to mention that the mechanical performance of the engine can also be represented by the Brake Mean Effective Pressure (BMEP) which is used to compare different engine, it is a sort of work per cycle of the engine normalised by the displacement V.

$$BMEP\ [bar] = 1200\frac{P_{eng}[kW]}{\omega_{eng}V[dm^3]} \qquad \textit{Eq. 11}$$

Another interesting parameter is the BSFC (Brake Specific Fuel Consumption) it is an intuitive parameter of engine efficiency, and it is expressed by Eq. 12.

$$BSFC\ \left[\frac{g}{kWh}\right] = \frac{1}{\eta_g H_i} \qquad \textit{Eq. 12}$$

It is used to create a sort of performance map for the engine, where are represented the iso-BSFC with BMEP or the engine torque on the y-axis, the engine speed on the x-axis.

4.5.2 Electric Machine

For HEVs powertrain development purposes, the map-based methodology is usually adopted for EM modelling, where its behaviour is described by means of torque and efficiency maps. A good correlation can be found between computed and experimental data. Due to the high speed at stake, the only modelled dynamic element is the rotor inertia. The relation between the input and the output power in EM can be simply obtained, as shown in Eq. 13:

$$P_{electric} = \frac{P_{mech}}{\eta(\omega, T)} = \frac{\omega \cdot T}{\eta(\omega, T)} \qquad \textit{Eq. 13}$$

Where $P_{electric}$ is the EM electrical power, P_{mech} the EM mechanical power, T the EM torque, ω the EM speed and $\eta(\omega,T)$ the EM efficiency depending on torque and speed.

The simulator used, presented in Section 4.7, models EM with loss maps for the electro-mechanical conversion and mechanical friction losses.

4.5.3 Battery

Electrochemical batteries are a key component of hybrid-electric vehicles (HEV).
Traction batteries are primarily characterised in terms of power, which has to match the power of the electric path, and nominal capacity, which has to match the desired driving range specification. The latter, usually expressed in Ah, is the integral of the current that could be delivered by a full battery when completely discharged under certain reference conditions.
A dimensionless parameter is the state of charge (SOC), which describes the capacity remaining in the battery, expressed as a percentage of its nominal capacity [32]:

$$SOC(t) = \frac{Q(t)}{Q_{max}} = \int_0^t \frac{i(t)dt}{Q_{max}} \qquad \textit{Eq. 14}$$

Where:

- $i(t)$ is the electric current instantaneously flowing into or from the battery;
- $Q(t)$ is the actual battery charge;
- Q_{max} is the maximum charge level.

For HEVs powertrain development purposes, a static model is usually adopted and it is also the one used in this analysis; i.e. a simple battery model, consisting in an equivalent circuit, where an ideal voltage generator is in series with a resistor (Thevenin approach). Dynamic behaviours during transient operating conditions are not considered [29].

The equivalent circuit adopted in this dissertation is shown in Figure 4.4 and consists of open-circuit voltage, internal resistance, and optional R-C branches for electrical dynamics. In this study, due lack of data, only the resistive branches were used.

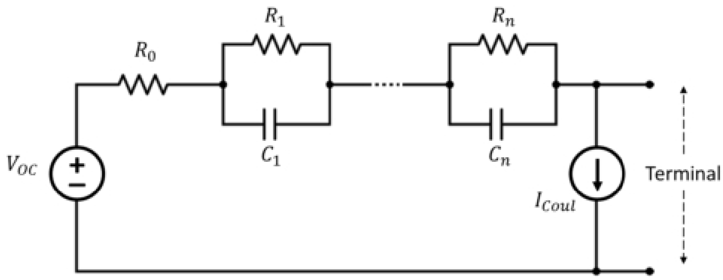

Figure 4.4 Electrical equivalent model of battery

4.6 Equations of motion

As seen in the previous paragraphs, for single components or subsystems development, detailed simulation models are usually implemented (e.g. 1D-CFD models for ICE or 3D-CFD models for in-cylinder phenomena). Instead, for an energy characterisation of hybrid vehicles, vehicle-level energy analysis is more suitable. A detailed 1D model will require high computational cost for assessing a vehicle fuel economy or pollutant emissions over long duration driving cycles. In the vehicle-level energy analysis, the vehicle is considered as a point mass, and the road load power is computed from its interactions with the external environment [30].

The equations of motion of a vehicle, considered as a point of mass, on an inclined plane have been achieved.

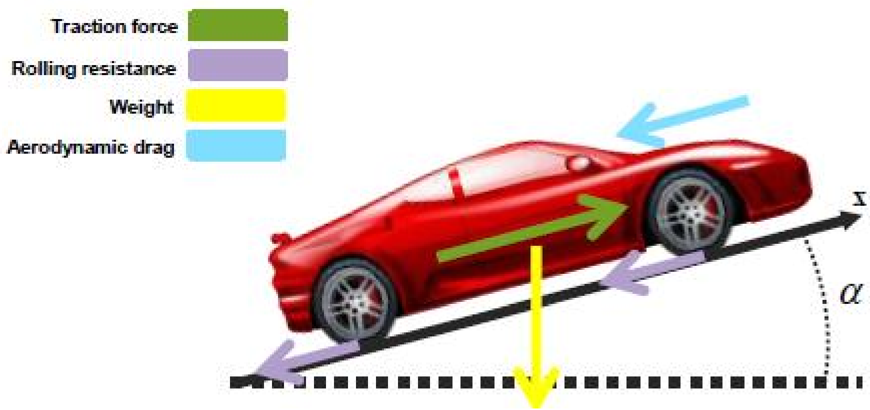

Figure 4.5 Forces acting on a vehicle [12]

To move the car, the power actuators must deliver force capable of counterbalancing the several forces acting on it. The equilibrium of forces applied on a general vehicle on an inclined plane [33]:

$$M_{eff}\frac{\overrightarrow{dv}}{dt} = \vec{F_t} + \vec{F_x} + \vec{R_s} + \vec{P} \qquad \textit{Eq. 15}$$

Where $\vec{F_t}$ is the tractive force, it is the sum of the forces acting on the individual wheels, and $\vec{F_x}$ is the aerodynamic drag that can be estimated as follow:

$$F_x = \frac{1}{2}\rho_a C_x A_f v_r^2 \qquad \textit{Eq. 16}$$

Where ρ_a is the air density, C_x is the aerodynamic drag coefficient,A_f is the frontal vehicle area and the v_r is the relative vehicle speed compared to air speed. The last three resistive forces are respectively the rolling resistance $(\overrightarrow{R_s})$, the resistance related to road slope $(\vec{P})$ and the inertial force $(M_{eff}\overrightarrow{\frac{dv}{dt}})$, all of them are directly proportional to the mass of the vehicle. The equation of motion, considering the vehicle as a mass point, can be written from the equilibrium of the forces:

$$M_{eff}\frac{dv}{dt} = F_t - R_s - F_x - P \qquad \textit{Eq. 17}$$

Otherwise, it can be rearranged to obtain the expression of the tractive force:

$$F_t = M_{eff}\frac{dv}{dt} + R_s + F_x + P \qquad \textit{Eq. 18}$$

4.7 Modelling Tools

The software used for implementing the simulator described in Section 4 is GT-Suite, a tool developed by Gamma Technology able to represent the behaviour vehicle driveline effectively with different detail levels. GT is a US company, the leader in the CFD simulation applied to the automotive field. All major engine manufacturers and their Original Equipment Manufacturer (OEMs) use its software for engine performance analyses, fuel injection systems and oil circuits simulations, vehicle thermal management analyses, driving cycle simulations, etc.

In this code, 1D fluid dynamic simulation can be performed. The engine can be represented by a set of elementary volumes, where the Navier-Stokes equations are solved in one dimension, providing average quantities across the flow direction. Moreover, heat-exchange processes, fluid leakages and mechanical losses can be depicted by sub-models. The implemented combustion models can simulate the chemical processes taking place inside the combustion chamber. The experimental trace of in-cylinder pressure can be simulated [34].

Furthermore, GT-SUITE can be used for performance, fuel economy and emissions analyses of a vehicle system. A set of standard driveline components and connections can be found in the *Vehicle Library*; different driveline layouts and configurations can be implemented and tested [35]. All the physical details are modelled, employing simple blocks containing their physical properties (lumped parameters models). Kinematic and dynamic 1D relationships are solved to simulate powertrain behaviour.

Since fuel consumption and energy flows are the main subjects of this study, backward kinematic approaches were adopted. The kinematic approach neglects all the dynamic phenomena; however, a high level of detail, able to describe the dynamic behaviour of each component of the powertrain, is not the objective of the present work. The implemented simulator in GT-SUITE is purely longitudinal: it does not take into account any lateral or vertical motion. Steady-state efficiency maps were used for modelling all the power sources (i.e. ICE, EMs). The kinematic analysis directly imposes the state (the speed) of a node on the driveline. This approach is in contrast to the standard dynamic analysis, the mode in which the engine (or alternative power source), driveline and vehicle accelerate freely under the influence of externally applied forces and torques.

Dynamic Programming has been performed, thanks to the specific functionality of GT-ISE. DP implementation in GT can be summarised into three steps [35]:

1. Calculation of transitional cost (forward marching in time). Given the profile of vehicle speed, transmission and EM brake torque, the controller determines the operating mode and the power split that should be delivered to the wheels, respecting the constraints. Then, using maps of the

components and feedback on their present state, it also determines the maximum and the minimum power that each energy source can deliver

2. Calculation of optimal cost-to-go or cumulative cost (Backward Marching in time). Once the grid of possible power splits, or solution candidates, is created, the procedure outlined earlier can be used, associating a cost to each of the solution candidates.
3. Retrieve optimal solution (forward marching in time). The optimal cost-to-go is calculated for each grid point, proceeding backwards from the end of the driving cycle and stored in a matrix of costs. When the entire period has been examined, the path with the lowest total cost represents the optimal solution.

5 Case studies

5.1 Test case

The case study is a Euro 6d-temp P2 Diesel Plug-In Hybrid Electric Vehicle (PHEV) already available on the market, and it is commercialized as Mercedes S300de. The ICE is a conventional 1950 cc Diesel engine, the EM is a 90 kW/440 Nm Permanent Magnet Synchronous electric motor, in P2 position. The hybrid powertrain is coupled with a 9-speed automatic transmission and a torque converter that transfer the torque to the rear wheels, according to a Rear-Wheel-Drive configuration. In Figure 5.1, it is possible to observe the assessment of the vehicle.

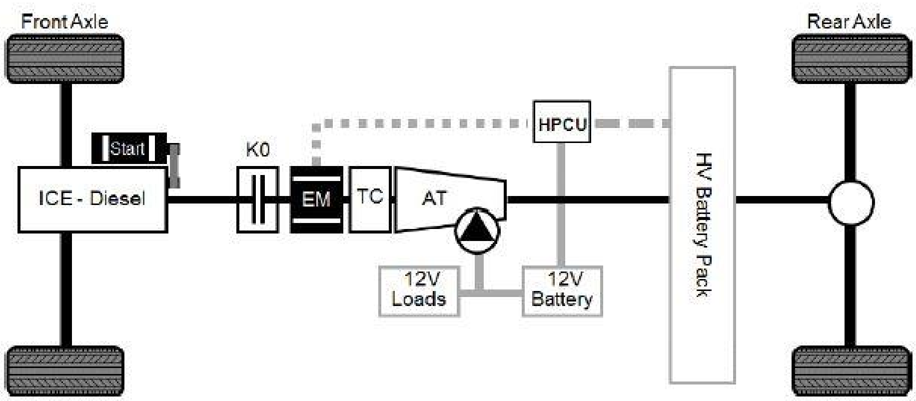

Figure 5.1 Powertrain schematics and main component [36]

The analysed vehicle is capable of driving in all-electric mode at a top speed of 130 km/h. Depending on the driver's demand, the four listed operating modes can be chosen [36]:

- **Hybrid Mode**: it is the default setting; all functions, such as electric driving, boost and energy recovery, are available according to the driving situation and route profile,
- **Electric mode (EV)**: electric driving by means of the main traction motor, for example in the city centre. The accelerator triggers the pressure point at which the combustion engine is started;

- **E-Save**: the HV battery is being recharged and held at a constant SOC to allow electric driving mode later;
- **Charge**: the battery is constantly charged while driving via the ICE load.

5.2 Experimental Campaign

The procedure [36] used to characterise the powertrain data used in this thesis consists of a novel reverse engineering methodology able to estimate relevant powertrain data required for fuel consumption-oriented modelling of the considered HEV. The vehicle and its main subsystems have been carefully instrumented, both on the thermal, electrical, hydraulic and mechanical side, to perform the powertrain characterization, as shown in Figure 5.2. Afterwards, the vehicle was tested on a chassis dynamometer under a specific test procedure which involves a limited number of tests, to explore different operating points and extract as much data as possible. The considered driving cycle was WLTC.

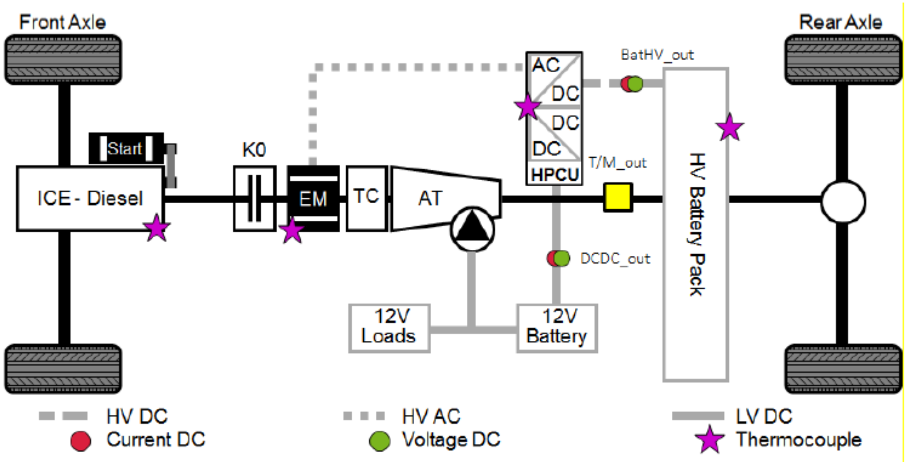

Figure 5.2 Powertrain layout with instrumentation details. Voltage and current sensors are used to measure the electrical power exchanged between battery and electric motor; a torque sensor on the propeller shaft measures the total torque coming out from the automatic transmission. The hydraulic pressures in the four brake calipers are measured and CAN data is logged [16]

The central part of the experimental test campaign was carried out with an All-Wheel Drive Chassis Dyno.

Once the chassis dyno had been set, the vehicle was placed on the test bench for the experimental campaign. Table 5.1 illustrates in detail the different types of tests performed for vehicle characterisation and their specific purpose. The Ramp-Up tests are carried out at constant and imposed vehicle speed, depressing the accelerator pedal by steps, for different gears in order to characterise transmission, electric motor and ICE efficiency. Constant Drive test is again performed at a constant speed but controlled by the driver as everyday on-road driving. Also, this test investigates different engine/EM load and speed, varying the selected gear. Finally, both Acceleration and Deceleration manoeuvres were carried out exploring different accelerator pedal positions or different deceleration rates via a suggested vehicle speed profile.

DYNO TEST	DESCRIPTION	SCOPE
Ramp-Up	Dyno steady speed, acc. pedal sweep, repeat for each gear	AT Efficiency EM Efficiency ICE Efficiency
Constant Drive	Steady speed	Battery Modeling
Acceleration	0-100 km/h different acc. pedal	Gearshift Threshold Torque Converter
Deceleration	Different constant deceleration levels	Braking System
Driving Cycle	WLTC	Overview Torque Converter

Table 5.1 Detailed test campaign for powertrain characterization [36]

The test campaign gathered essential data for powertrain characterisation of the vehicle that are: the AT efficiency, the efficiency of both the EM and the ICE, the HV battery circuit, the torque converter main physical parameters, the braking system behaviour and, finally, the gearshift threshold maps.

The creation of efficiency maps for the transmission, the EM and the ICE, constitutes a valuable dataset [36] that is inserted in this study into the map-based vehicle model for the assessment of the vehicle. Moreover, the methodology can map the equivalent values of both the OCV and battery internal resistance for the complete battery pack. Furthermore, the gearshift thresholds have been found for gears from the 1st to 5th; unfortunately, the other gears could not be analysed.

Finally, with the aid of simple instrumentation on the braking system, the main characteristic of the vehicle behaviour during deceleration phases have been found. Part of these values is used in this study to characterize the performance of the vehicle.

5.3 GT-SUITE embedded Dynamic Programming

5.3.1 Model Setup

The test case was developed in order to investigate the performance of the DP optimisation toolbox integrated into the GT-SUITE v2020. The embedded DP routine need to work a simplified vehicle model. Therefore, a kinematic model of the high-performance hybrid electric vehicle was built for the DP functionality compatibility (Figure 5.3). The connection between ICE and EM was obtained by means of a clutch, and the ICE can be decoupled and forces to switch off when not needed thanks to a clutch controller. Control logic for the gear shifting was implemented with TransControl template. The VehKinemAnalysis folder is used in conjunction with the vehicle driveline model, and it allows to activate the kinematic analysis modes, in which a known speed history is imposed on the driveline model.

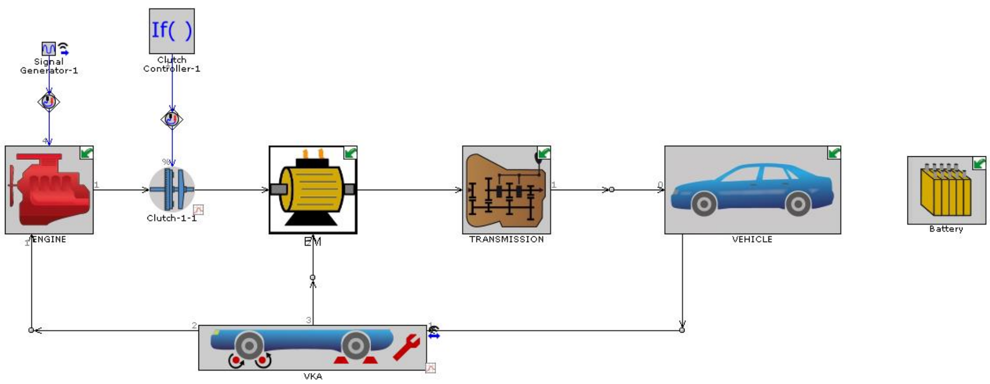

Figure 5.3 Simplified vehicle model

5.3.2 Model validation

Before assessing the capabilities of the DP toolbox, the model has to be validated against the experimental data in order to verify that it is able to replicate the real model physics. For this purpose, the backward kinetic model with imposed vehicle speed and gear profiles has been set (Figure 5.4) to analyse the efficacy of the GT model. The realisation of a model that represents the dynamic of the vehicle is out of the scope of this analysis, the scope of the validation is only to have a suitable model for the DP implementation. In order to avoid any errors due to coding also the MGU torque and the engine state profiles have been set in the simulator. The speed, gear profiles, the MGU torque profiles and the engine state profiles have been set equal to experimental data, acquired in the experimental campaign (Section 5.2), related to the two driving cycles: NEDC and WLCT. The SOC is dynamically calculated based on electrical demand. Once obtained the results, the comparison between the experimental data and the simulation data has been made to assess the validity of the model.

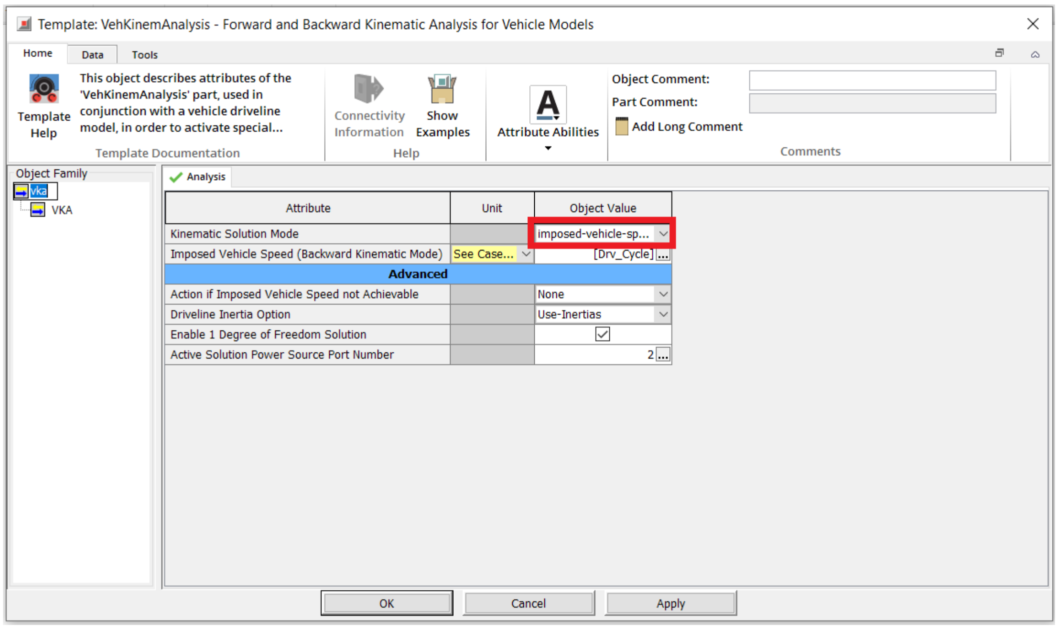

Figure 5.4 VehKinemAnalysis Template during validation phase

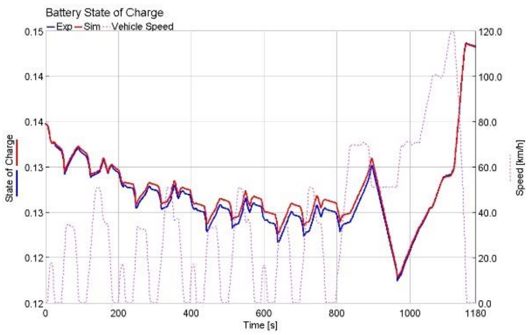

Figure 5.5 SOC during NEDC in the validation phase

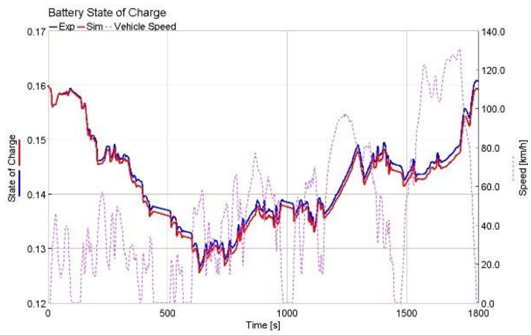

Figure 5.6 SOC during WLTC in the validation phase

Figure 5.5 and Figure 5.6 show respectively, the State Of Charge during NEDC and WLTC. The red line represents the simulated data acquired with GT, while the blue line represents the experimental data. The lilac line depicts the vehicle speed profile. The adopted colour scheme is the same in all plots used in the comparison. During both driving cycles, the simulated data overlap almost perfectly the experimental ones.

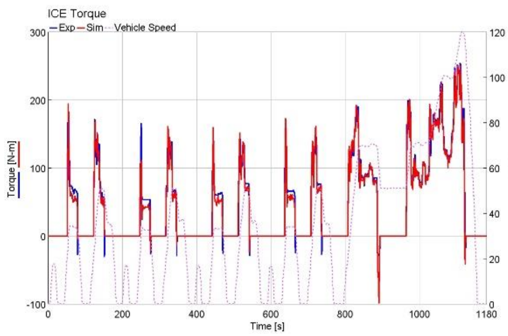

Figure 5.7 ICE torque during NEDC in the validation phase

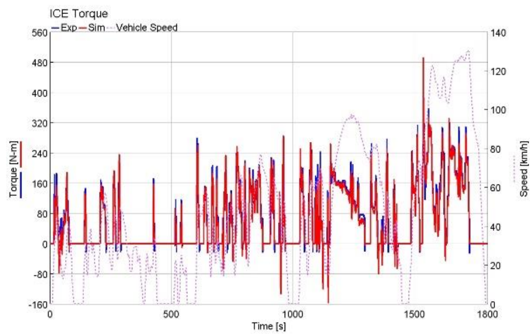

Figure 5.8 ICE torque during WLTC in the validation phase

Figure 5.7 and Figure 5.8 illustrates the ICE torque in both mission profiles. It is possible to observe that the results obtained with GT code present some spikes, especially during WLTC, these errors are due to the accuracy of the simulation process, and they can be considered acceptable.

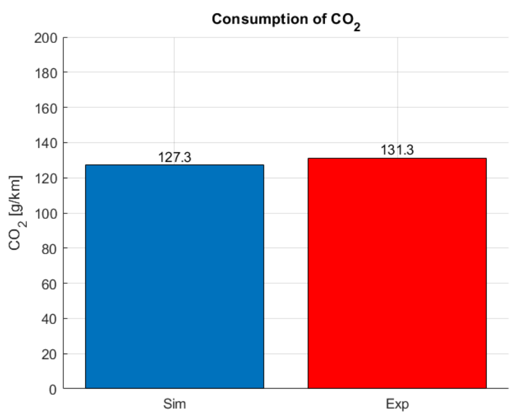

Figure 5.9 CO2 consumption in g/km during NEDC

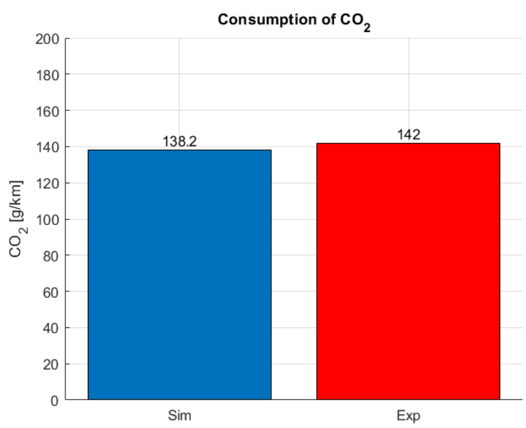

Figure 5.9 CO2 consumption in g/km during WLTC

Figure 5.8 and Figure 5.9 represent the CO_2 consumption in the two cycles. The differences between the simulation and the experimental results are very small. Taking into account the results obtained, the model can be considered valid to represent the performance of the vehicle, and it is suitable for DP implementation.

5.3.3 Dynamic Programming implementation

To enable the Dynamic Programming optimisation, it is sufficient to change some option in the VKA template by choosing the *Backward-State-Optimization* in the *Kinematic Solution Mode* option like shown in Figure 5.10.

The considered state variable is the SOC. The cost of policy u, starting at initial condition $x_o = SOC(0)$, is:

$$J_\pi(x_o, u) = g_N(x_N) + T_N(x_N) \ldots + \sum_{k=0}^{N-1} L_k\big(x_k, u_k(x_k)\big) + p_k(x_k) \qquad \textit{Eq. 19}$$

Where $g_N(x_N) + T_N(x_N)$ is the final cost. First term $g_N(x_N)$ corresponds to the terminal cost. Second term $T_N(x_N)$ is an additional penalty function forcing a partially constrained final state, named Terminal State Penalty (T_N) that is calculated in this way:

$$T_N = \gamma * \left(SOC_{grid} - SOC_{des}\right)^\beta \qquad \textit{Eq. 20}$$

Where:

- γ = Terminal State Penalty Weight,
- β= Terminal State Penalty Exponent,
- SOC_{grid}=discretized SOC points bounded by Maximum and Minimum Battery SOC
- SOC_{des}=Target Battery SOC
- $L_k\big(x_k, u_k(x_k)\big)$ is the instantaneous cost function
- $p_k(x_k)$ is the penalty function that helps to stays in the discretized interval $[SOC_{min}, SOC_{max}]$; in the case of DP, GT-SUITE calculate it as follow:

$$p(SOC) = \lambda * \left(\frac{SOC(t) - SOC_o}{\frac{SOC_{max} - SOC_{min}}{2}}\right)^\alpha \qquad \textit{Eq. 21}$$

Where:

- SOC_o= target SOC
- SOC_{max}= maximum battery SOC
- SOC_{min}= minimum battery SOC
- λ= penalty function weight
- α= penalty function exponent.

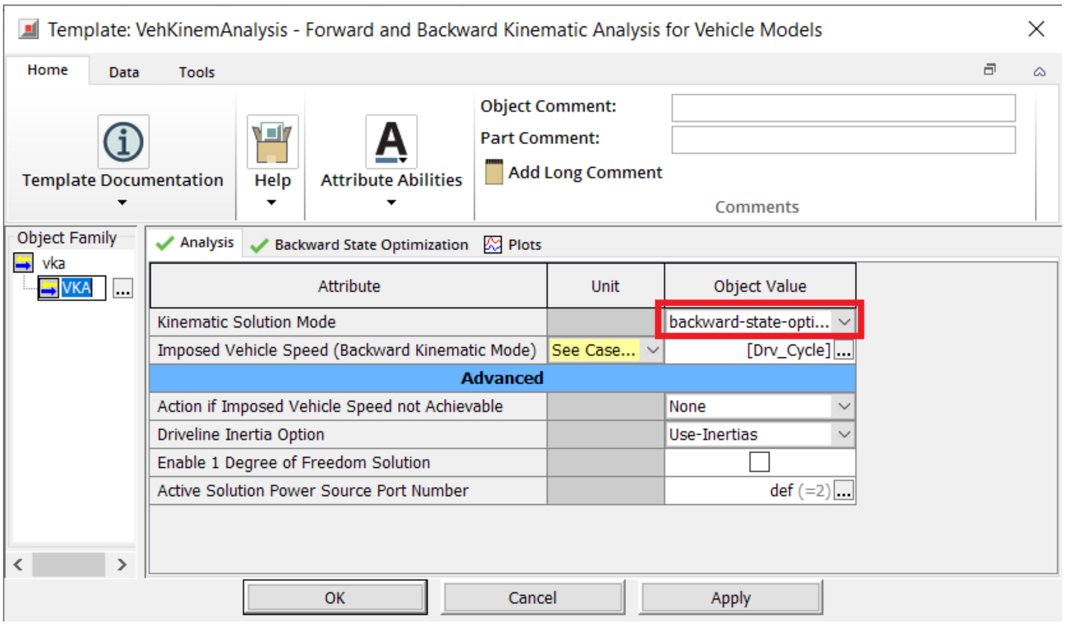

Figure 5.10 VehKinemAnalysis Template

By opening the *VehStateOptimization* object in the *Backward State Optimization* folder, the DP features should be selected (in orange in Figure 5.11). In this object, the state variable, its limits and the targets are introduced (in red), and the cost and penalty function can be defined (in blue).

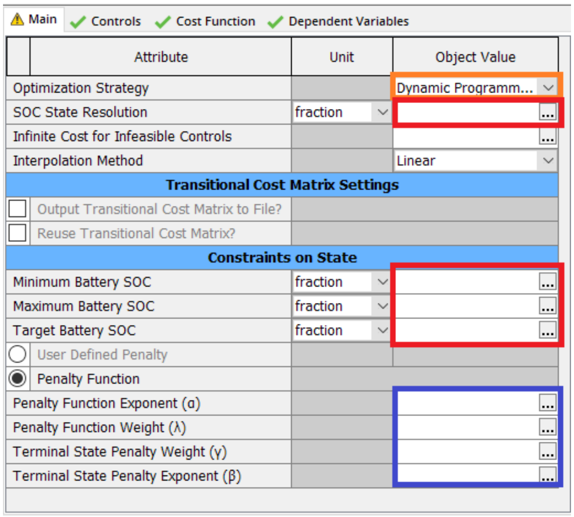

Figure 5.11 VehStateOptimization Main folder

The SOC State Resolution attribute determines the discretization of state - State of Charge (SOC). A larger resolution will cause the optimizer to take fewer total iterations, thereby allowing a solution to be found faster, but the final solution will be less precise. It has been chosen a value of SOC_{res} that allows a compromise between the accuracy and the computational time. This is applied to the range determined by Maximum Battery SOC and Minimum Battery SOC. The Infinite

Cost for Infeasible Controls value is the cost applied to infeasible controls. Infeasible controls are the controls that lead to violation of dependent variables constraints.

The penalty function attribute has been set equal to zero in this study because with DP there is no risk to go out the SOC admissible region. At this scope, λ has been fixed equal to zero, and the value of α has been ignored.

The only parameters we had to set were γ and β. These values serve to calculate the Terminal State Penalty (Eq. 20). In order to choose the correct values of γ and β an iterative optimization has been performed with the aim to achieve at the end the target SOC without too high computational cost. Figure 5.12 illustrates the SOC profile with three different values of gamma, maintaining equal all the other settings. The red line represents the chosen gamma, and the blue and green lines are respectively obtained with +10% and -10% of the reference gamma. Figure 5.13 shows the zoom of the circled part of the Figure 5.12, it is highlighted that the SOC profile with the chosen value (red line) realises the perfect Charge Sustaining.

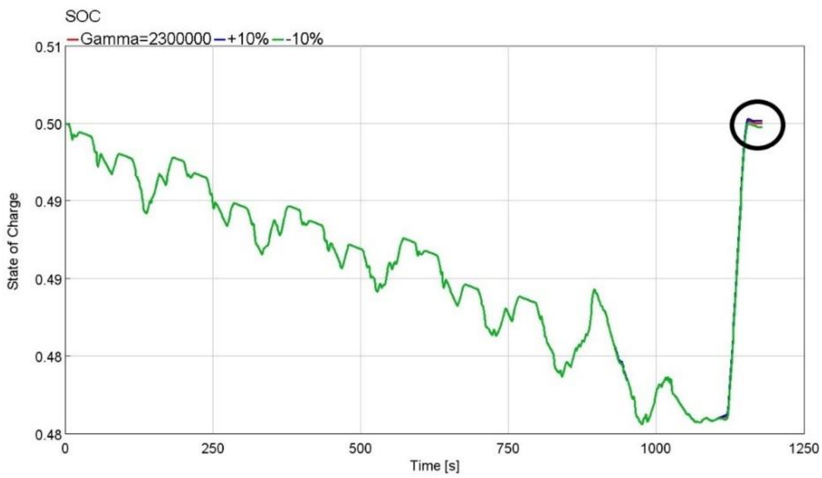

Figure 5.12 State of Charge during NEDC with different values of gamma

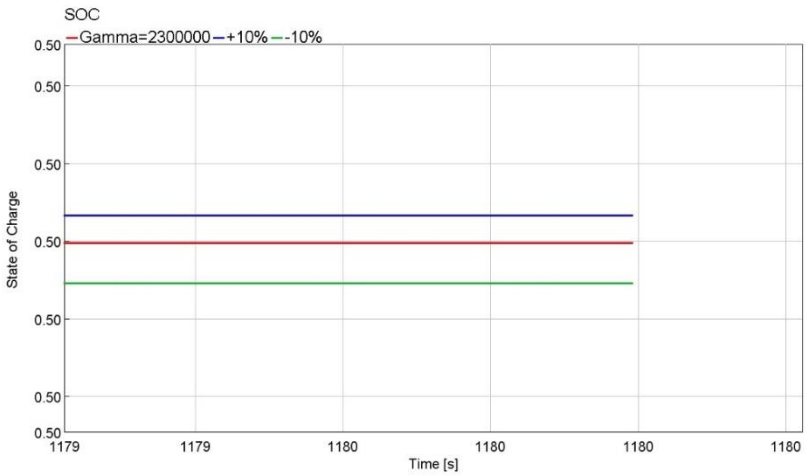

Figure 5.13 Zoom of State of Charge during NEDC with different values of gamma

The exponent β can assume only integer value. It is possible to observe in Figure 5.14 that it is necessary an even value since the base of the exponent is negative (Eq. 20). It is evident that β=2 is the best choice.

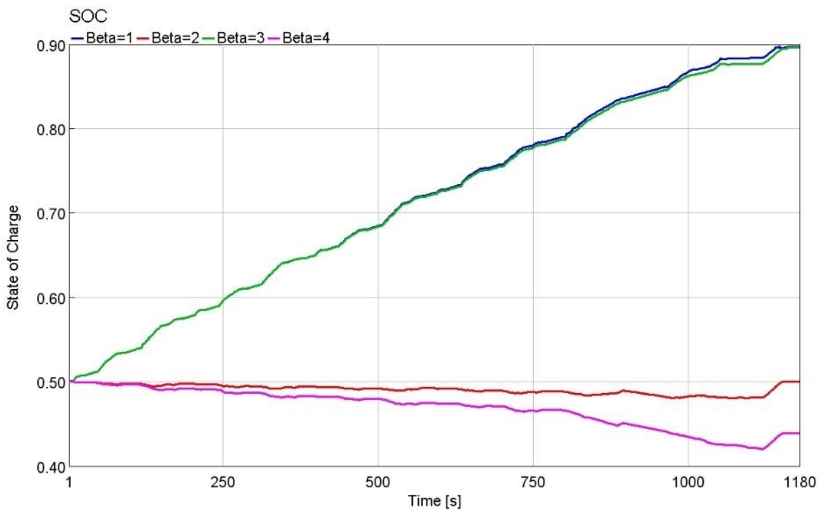

Figure 5.14 State of Charge during NEDC with different values of beta

In the *Controls* object are specified the control variable for the backward state optimization function that in this case is the vector $u(\mathrm{t}) = [Pow_{source}, Torque_{MGU}]$. The Pow_{source} represent the active power actuator, so the operating mode adopted by the DP (Parallel Mode or EV mode). The $Torque_{MGU}$ is the electric motor torque. Both the state SOC and the controls u are bounded as it is possible to observe respectively from Figure 5.11 and Figure 5.15. The SOC is limited in the range of 20%-90% in order to avoid deep cycling. The deep cycling represents the phenomenon of electrodes damage due to the fully discharged or recharged. The active power source can assume only two values, the number 2 means the thermal engine, and the number 3 represents the electric machine. The EM torque is limited in the range of the maximum and minimum torque of the considered engine that is [-440 440] Nm. The resolution value represents the precision of the optimized independent variable.

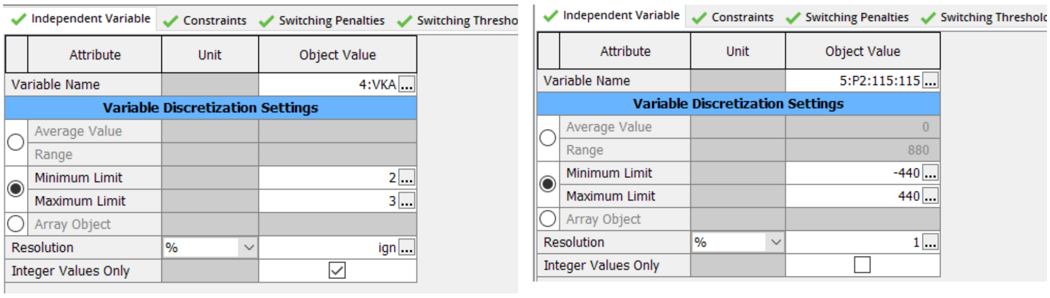

Figure 5.15 VKA: Independent Variable Setting

In the *Cost Function* folder, the *Default* cost function is used that involves Fuel in grams, minimizing the fuel rate consumption. In the *Dependent Variable* folder, constraints have been set up on Electric Motor Torque in order to avoid that it exceeds the limits.

In the first instance, it has been imposed through an external controller that the thermal engine must be off during deceleration phase for avoiding unrealistic behaviour even if more convenient for the Fuel Consumption perspective.

5.4 Results

5.4.1 NEDC & WLTC

Once the CS condition is guaranteed through a proper calibration of γ and β parameter, the main simulations could be performed. In Figure 5.16 the SOC trend during the NEDC and WLTC are plotted.

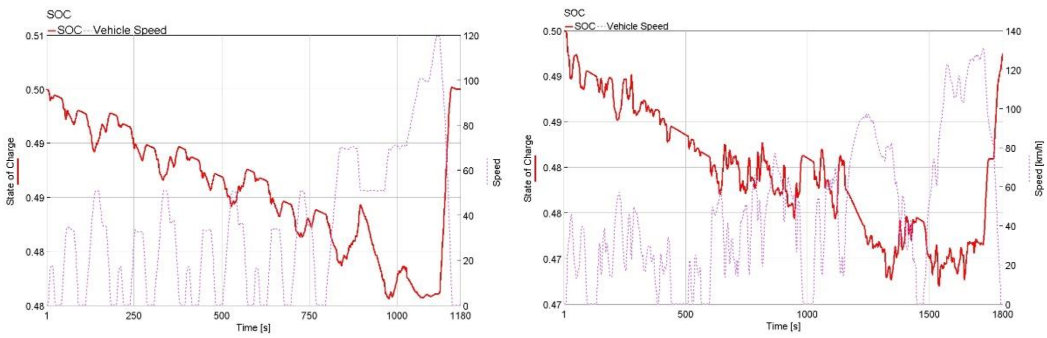

(a) State of charge during NEDC *(b) State of charge during WLTC*

Figure 5.16 DP State of charge during (a) NEDC and during (b) WLTC

Generally, the DP discharges the battery in the first part of the driving cycles, and it restores the initial SOC charging it at the end of the cycles to achieve the Charge Sustaining. This strategy could be performed by the DP thanks to the knowledge of the driving cycle: the DP discharges the battery in the early stage of the mission profile where the engine is inefficient and recharges it in the last deceleration.

The battery is being discharged during acceleration phases because the EM works as an actuator, instead of during the deceleration phase the battery is being charged thanks to the reversed direction of EM current, that works as a generator.

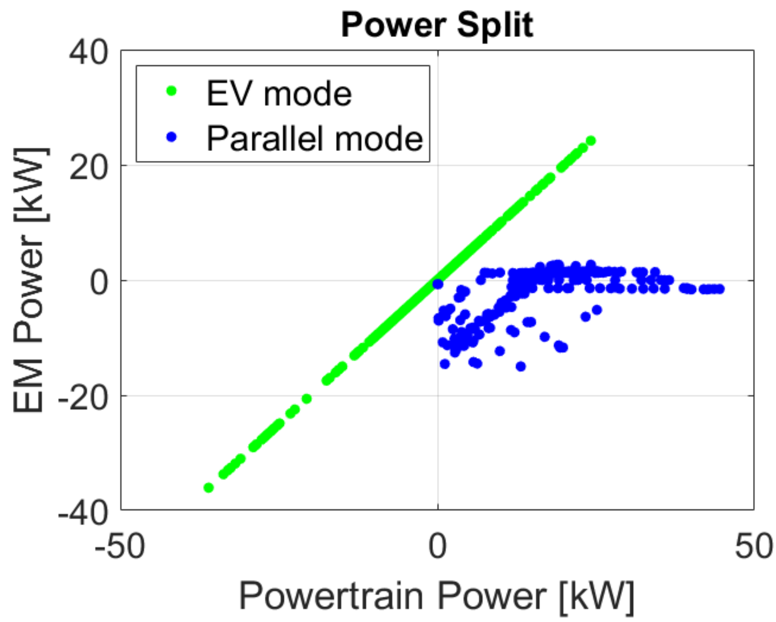

Figure 5.17 DP power split during NEDC

It is possible to see on Figure 5.17 that DP power split during the NEDC; in parallel mode the EM works mainly in load point moving to recharge the battery, instead of operating as an e-booster.

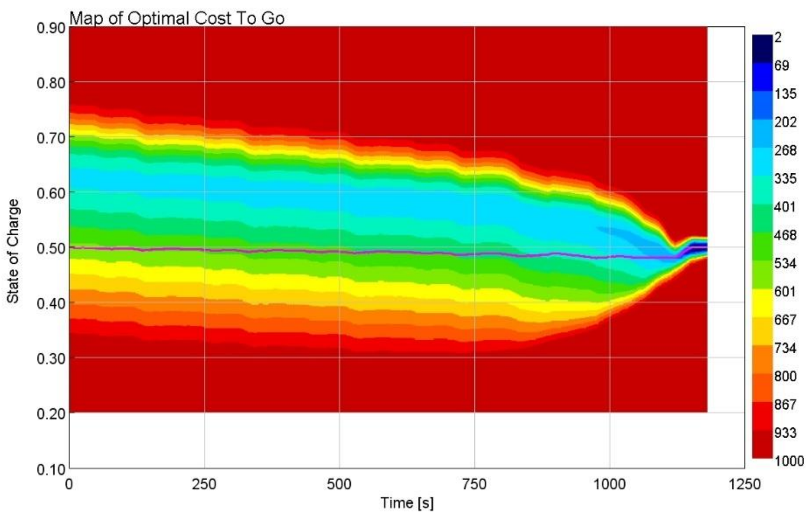

Figure 5.18 NEDC: Map of Optimal Cost To Go

The GT processes the map of Optimal Cost To Go that represents the map of the cost-to-go function (see Eq. 10) computed in backward for each value of the SOC in the acceptable range. The map is illustrated in terms of time, on X axis, and SOC, on Y axis. Thanks to this map (see the example of NEDC in Figure 5.18) it is possible to prove that DP procedure is able to select the SOC optimal sequence that minimised the cost-to-go. The reason why the SOC line is not always present in the light blue area lies in the other set constraints.

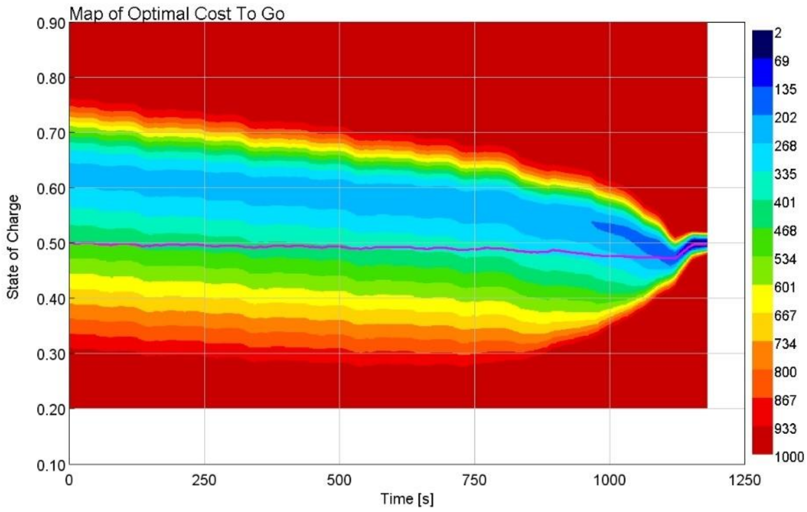

Figure 5.19 NEDC: Map Of Optimal Cost To Go without the constraint on the ICE

It is possible to see in Figure 5.19 that by removing the external controller on the thermal engine during the deceleration phases, the DP is able to maintain the SOC in a sequence that further minimized the cost-to-go.

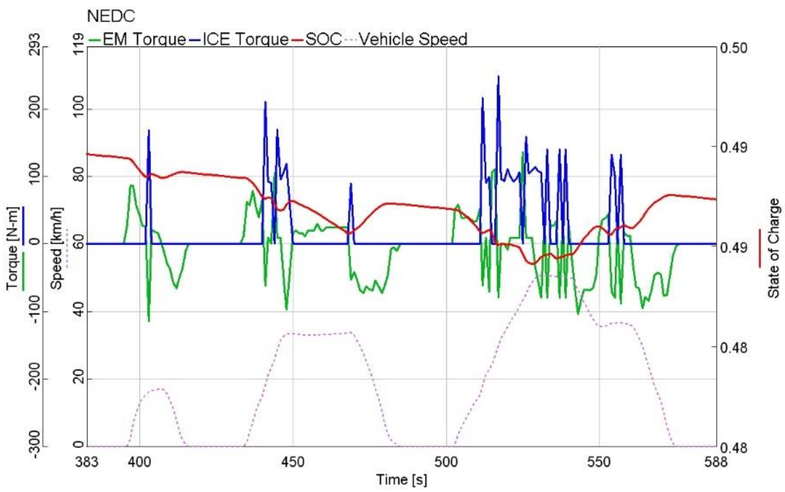

Figure 5.20 NEDC: Urban Driving Cycle

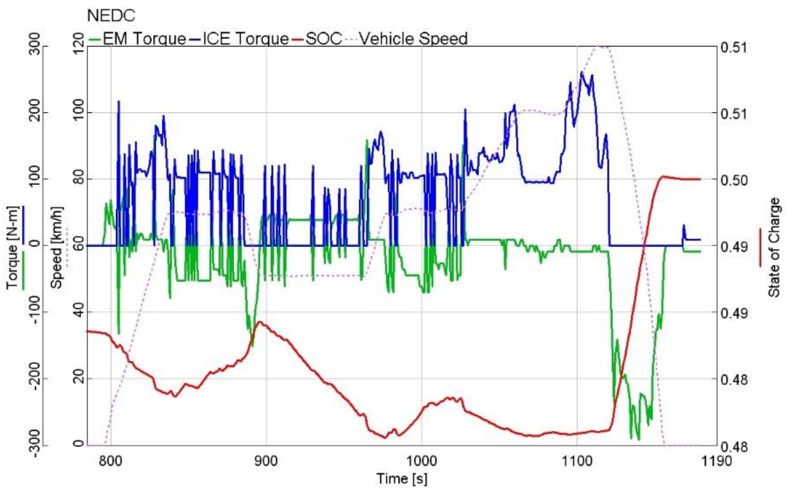

Figure 5.21 NEDC: Extra Urban Driving Cycle

Figure 5.20 and Figure 5.21 represent the focus on one Urban Driving Cycle and the Extra Urban Driving Cycle of the NEDC. It is possible to observe that the ICE torque, depicted in blue, is almost always equal to zero during the Urban Driving Cycle because of its low efficiency, while, during the Extra Urban Driving Cycle delivers positive torque for most of the time, except when the vehicle decelerates. The EM torque, represented in green, provides negative torque to recharge the battery when the engine is ON, implementing a load point strategy.

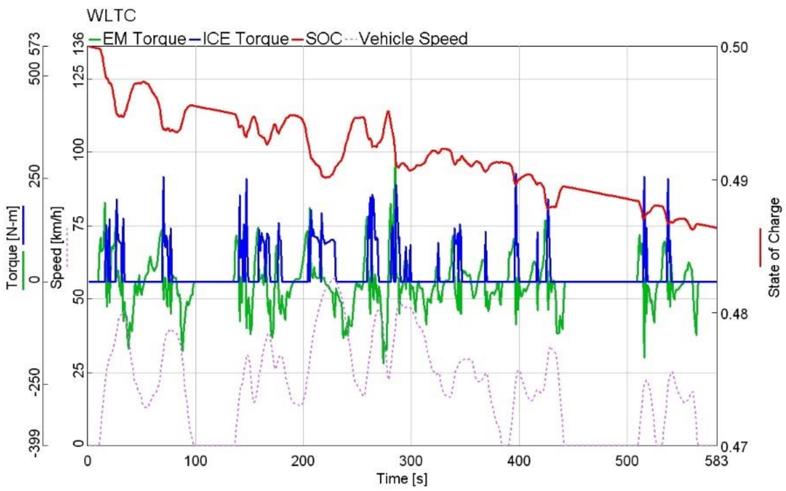

Figure 5.22 WLTC: Low phase

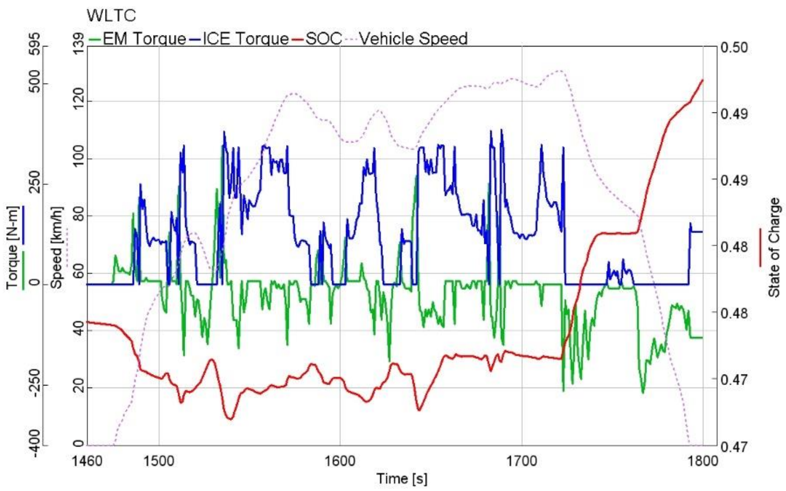

Figure 5.23 WLTC: extra-high phase

Figure 5.22 and Figure 5.23 show what happens in the low and extra-high phases of the WLTC. As in the NEDC cycle, ICE delivers high positive torque during acceleration phases and during with high speed phases, while, the EM recharge the battery mostly during deceleration phases. The EM ensures, also in this case, to ensure the CS.

It turns out from the experimental data that the Rule Based strategy adopted by the manufacturers consists of a Charge Depleting-Charge Sustaining approach. When the battery is completely charged the PHEV operates most of the time in EV mode while the internal combustion engine is exploited only if the power request exceeds the maximum performance of the EM. As a result, the battery is gradually depleted up to a minimum level where the vehicle switches to CS mode. In this condition, the thermal engine becomes the primary power source to drive the vehicle while the electric motor is used to realize a load point moving strategy maximizing the engine efficiency. It is possible to verify this strategy from Figure 5.24 that illustrates an experimental SOC trend, got applying a RDE.

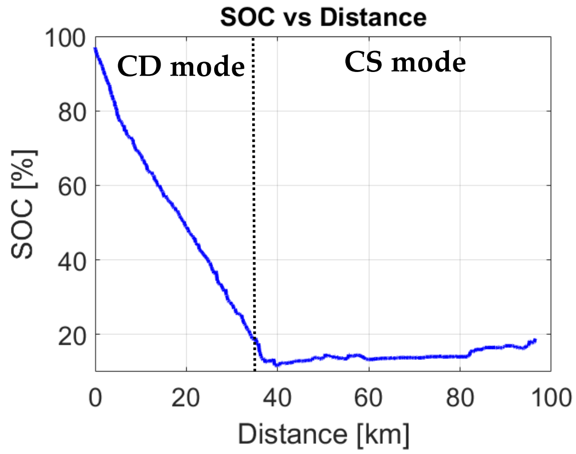

Figure 5.24 SOC with RDE

Assuming the same CD+CS high level approach, the control law defined by the DP has been compared with the real strategy obtained from the experimental test. The comparison has been made on NEDC, WLTC and RDE driving cycles considering only the CS part of the mission profiles to highlight the Dynamic Programming advantages from a Fuel Consumption perspective. DP simulations have been performed with the same initial SOC, vehicle speed and gear profiles of the corresponding chosen cycles.

Figure 5.25 and Figure 5.26 show respectively the SOC trends during NEDC and WLTC of the two different simulations. The red line represents the SOC with DP routine, while the green line is the Rule Based results. It is possible to observe that with both implementations, a similar swing of SOC is obtained. In low vehicle speed regions, more amount of battery energy is being used, leading to a drop in SOC up to 3% from its initial state and then during the end of the driving cycle where speed is high, the engine is used thanks to its higher efficiency at higher speeds. Hence, the motor provides negative torques, thereby shifting the engine load to the more efficient operating region while ensuring both the battery recharge and the power to drive. The reason for the similar trends lies in the same aim of minimizing fuel consumption.

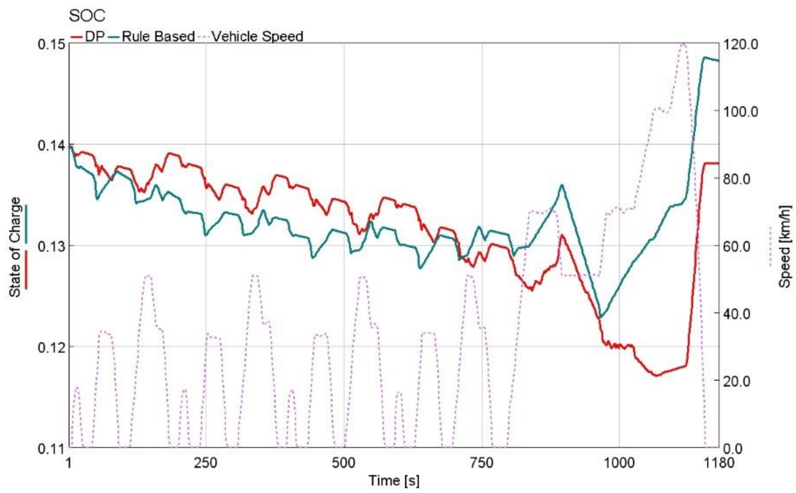

Figure 5.25 NEDC: SOC trends of Rule Based and DP models

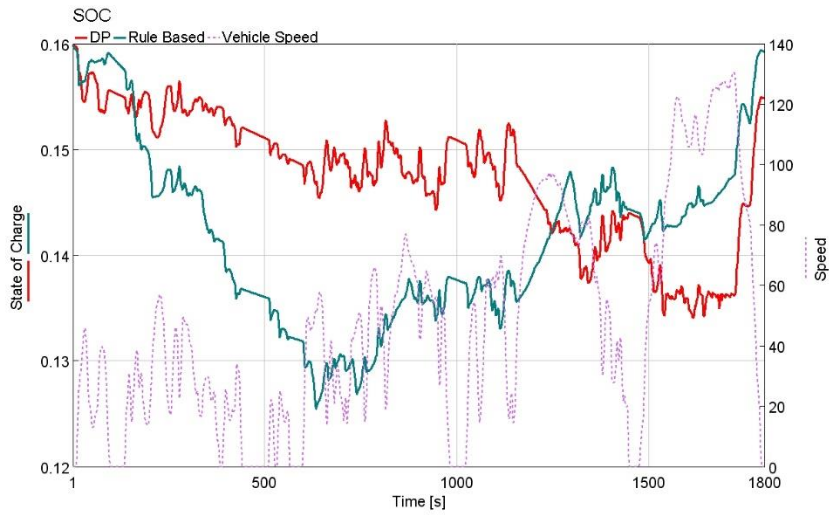

Figure 5.26 WLTC: SOC trends of Rule Based and DP models

In both cases, the energy of the battery is recovered in the abrupt decelerations, and it is used to boost the vehicle during the accelerations. A further analysis was aimed at investigating how the embedded DP manages the power split among the actuators. The plots on the left represent the results of simulations with a real strategy, while the figures on the right represent the obtained results with DP routine. In the WLTC driving cycle, the difference between the two strategies is more evident. The RB strategy discharges the battery immediately and recharges it for the remainder of the cycle, while the WLTC maintain a certain level of SOC in the intermediate phase and discharge the storage at the end of the cycle, when the power request is higher.

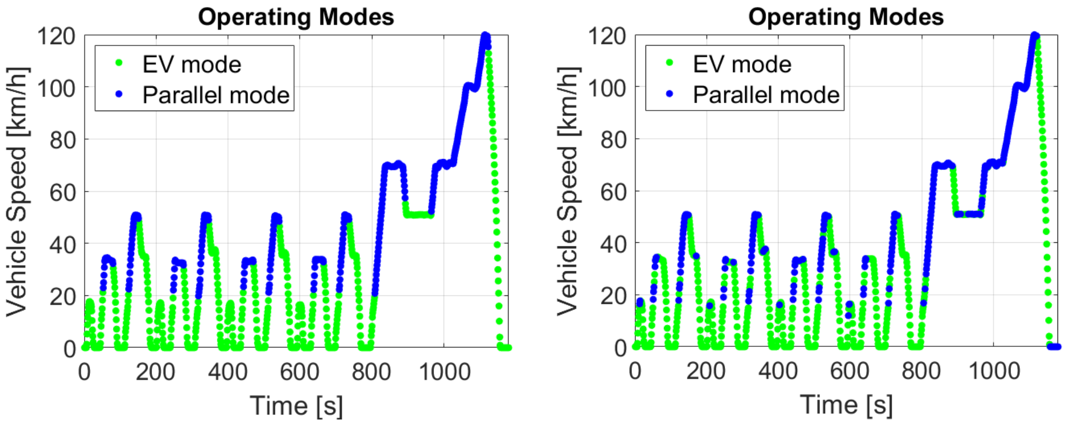

(a) *(b)*

Figure 5.27 NEDC operating modes with (a) Rule Based strategy and (b) DP strategy

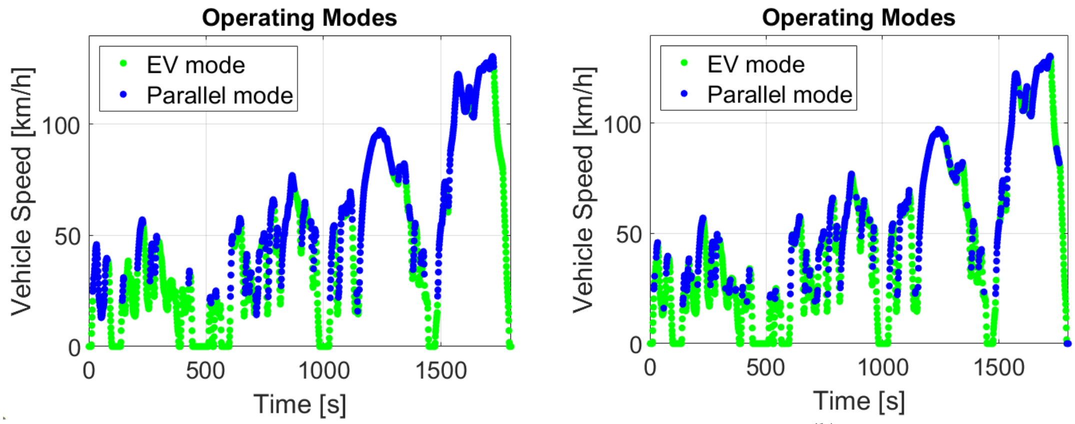

(a) *(b)*

Figure 5.28 WLTC operating modes with (a) Rule Based strategy and (b) DP strategy

In Figure 5.27 and Figure 5.28 the operating modes are reported on the speed profile. The drive-away is in EV with both strategies; there are small differences between the RB and DP strategies from operating modes point of views. In both cases, the strategy, for most of the time, drive the vehicle in Parallel mode during the acceleration phase and in EV mode during the deceleration one. The RB strategy is very close to the optimal result.

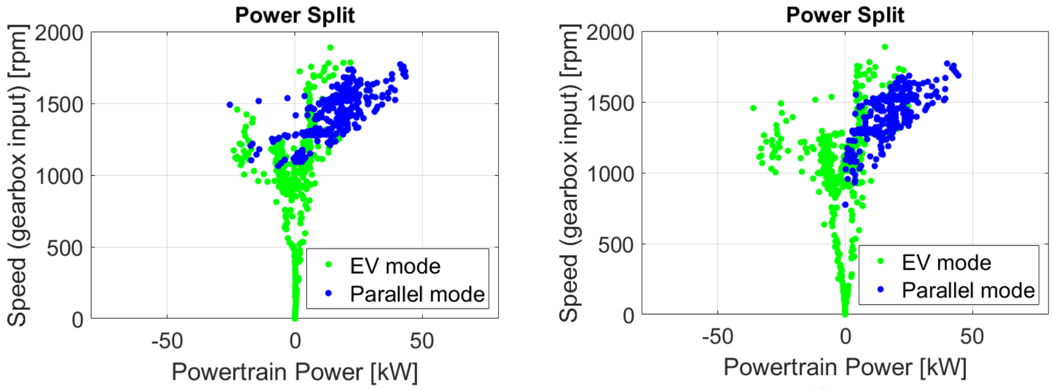

(a) *(b)*

Figure 5.29 NEDC power split with (a) Rule based strategy and (b) DP strategy

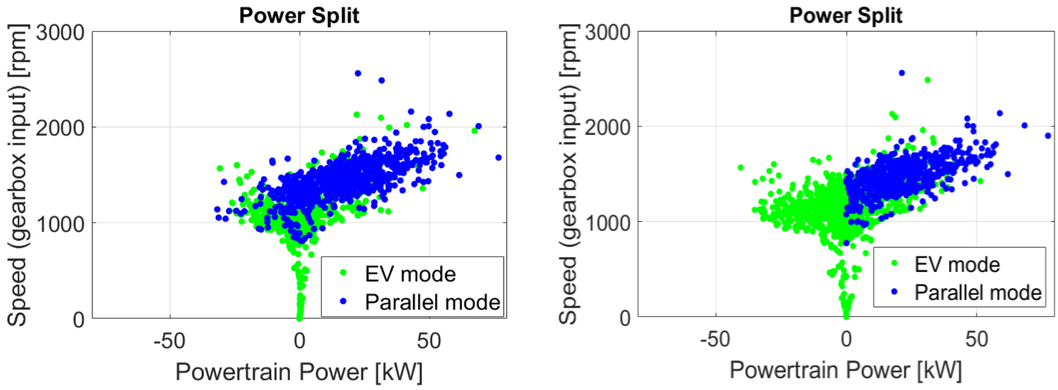

(a) *(b)*

Figure 5.30 WLTC power split with (a) Rule based strategy and (b) DP strategy

Figure 5.29 and Figure 5.30 illustrate the different operating modes in terms of total power of powertrain provided to the wheel and the rotational speed at the input of the gearbox. The embedded DP let to use the ICE mainly at powertrain speed higher than 1000 RPM and with positive power. It is possible to observe in the DP power split that the EM works at higher negative power. The Global Optimisation exploit the ICE only in the high-efficiency area, utilizing the ICE as an auxiliary power generator that delivers power when the EM exceeds the maximum performance.

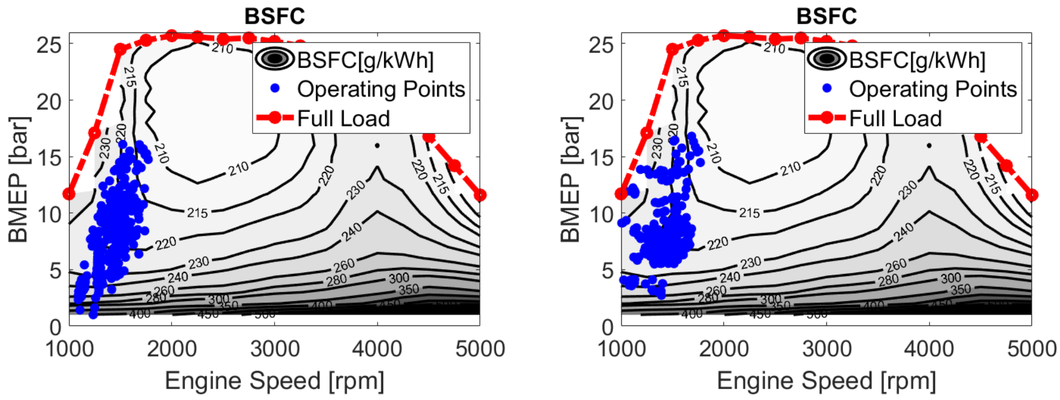

(a) *(b)*

Figure 5.31 ICE operating points during NEDC obtained with (a) Rule based strategy and (b) DP strategy

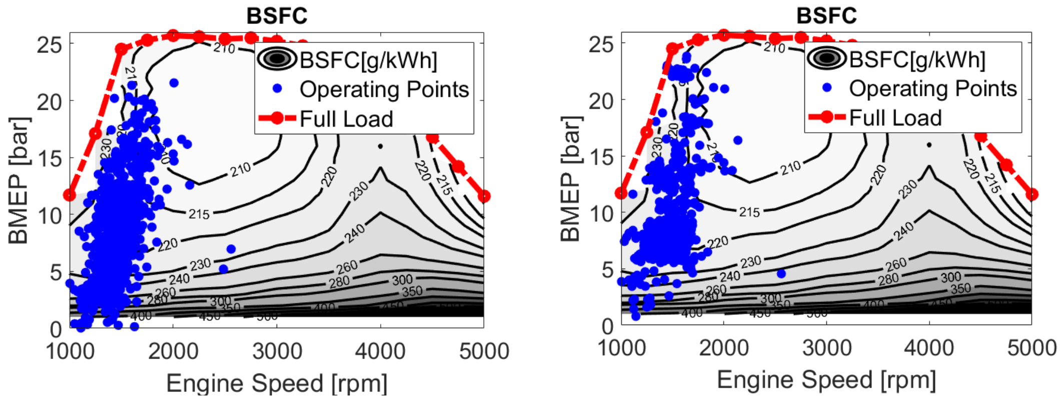

(a) *(b)*

Figure 5.32 ICE operating points during WLTC obtained with (a) Rule Based strategy and (b) DP strategy

In Figure 5.31 and Figure 5.32, the ICE operating points respectively during NEDC and WLTC with the two considered strategies are plotted on BSFC map. It is eye-catching that the introduction of DP reduces the number of ICE operating points especially in the low efficiency region since it supports the ICE traction only during phases with high power demand. It is possible to observe that there is not significant change in the distribution of the operating points from the speed perspective between the two different simulations. The reason for the same trends lies in the imposed equal gear profile in both conventional and DP simulations.

The Dynamic Programming procedure permit to have the global optimum in terms of fuel consumption. It is possible to observe in Figure 5.33 and in Figure 5.34, that DP optimization allows have a reduction of fuel consumption of respectively 13.5% during NEDC (Figure 5.33) and 9.3% during WLTC (Figure 5.34).

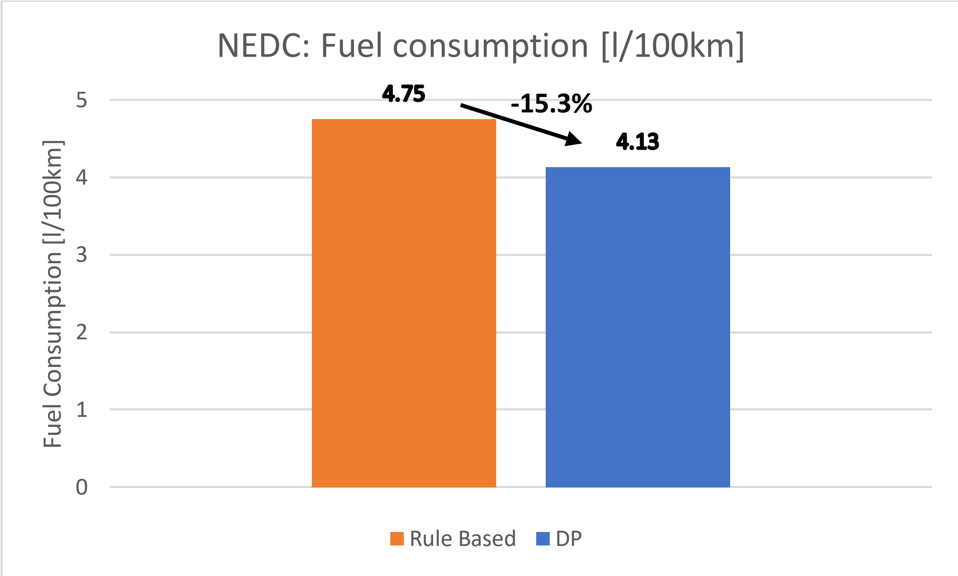

Figure 5.33 NEDC: Fuel consumption

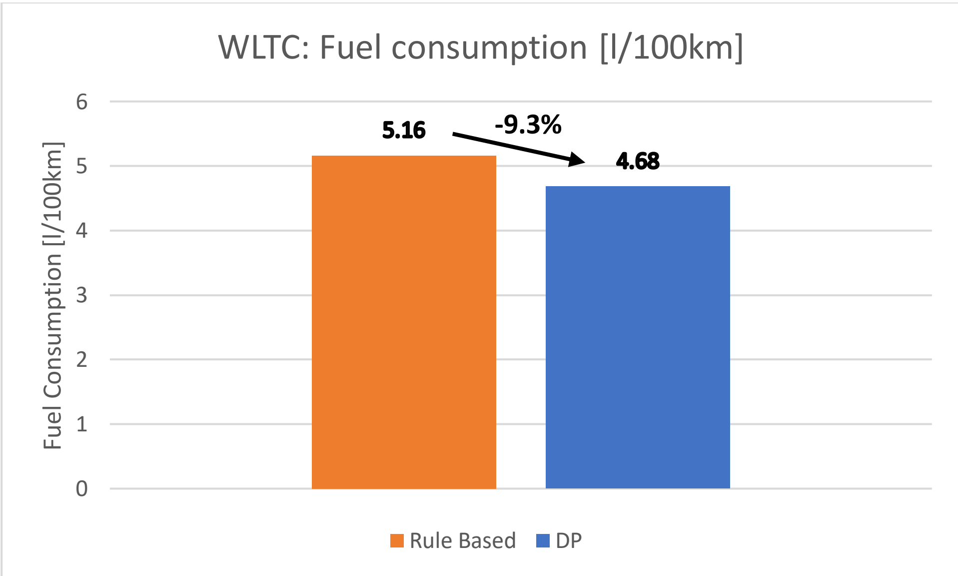

Figure 5.34 WLTC: Fuel consumption

From the results reported, the GT-SUITE embedded DP has demonstrated to perform the global optimal energy management strategy providing a significant enhancement of the vehicle fuel economy despite the RB control law is not so different. Analysing the DP results, some simple rules can be developed to optimise the rule-based strategy adopted on a real vehicle. These rules regard mainly the thermal engine state, which is expected since the fuel reduction is the first target of the optimisation. Analysing the power split plot regarding the NEDC, it is possible to outline the region where the DP allows the ICE to switch on (Figure 5.35).

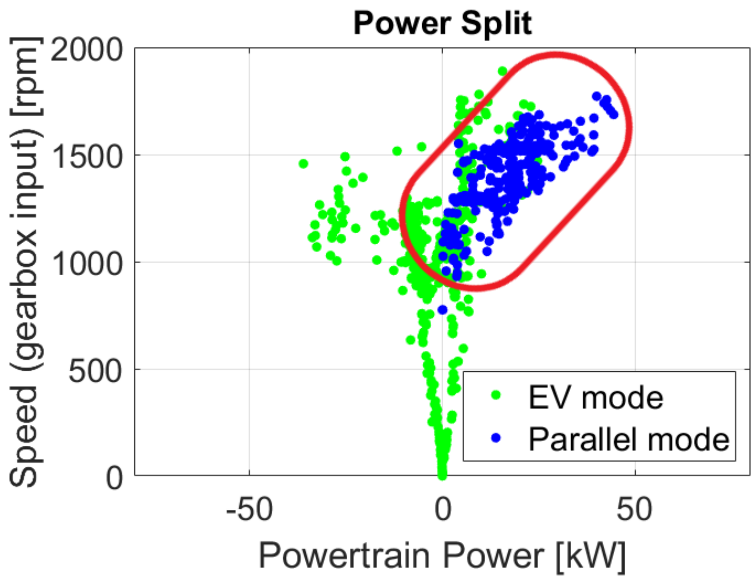

Figure 5.35 NEDC power split: area with ICE on

The DP routine allows to switch on the ICE only with gearbox speed higher than 1000 rpm and positive power. To optimise the energy management strategy of the vehicle from a fuel consumption perspective it should be necessary to integrate this simple law that consists in delivering ICE power only in its high-efficiency area, the region with positive power and gearbox speed higher than 1000 rpm and where the power and gearbox speed.

5.4.2 RDE

Dynamic Programming has been also applied to a RDE. The global optimisation has been implemented only on the part of the driving cycle in Charge Sustaining here too. The vehicle speed profile of the analysed part of the driving cycle is presented in Figure 5.36.

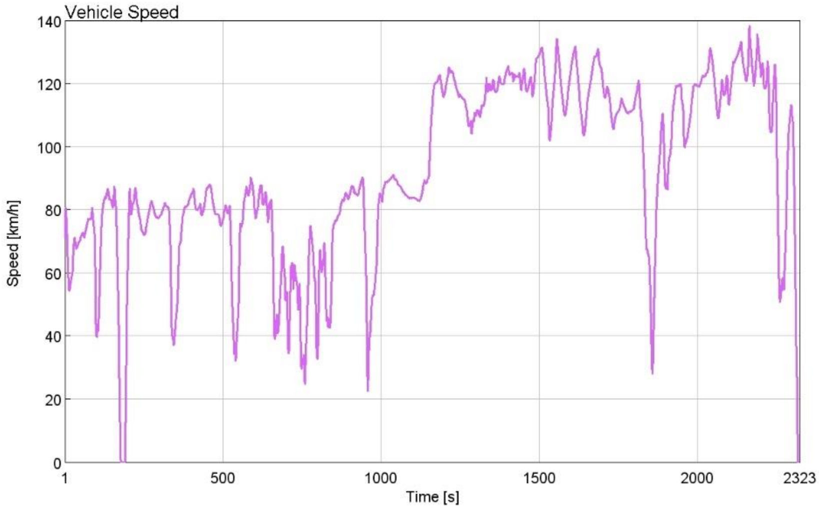

Figure 5.36 RDE vehicle speed

Differently from the NEDC and WLTC cases, with RDE the code does not allow to impose the external control on the regenerative braking of ICE due to the too high computational cost caused by the more complex driving cycle.

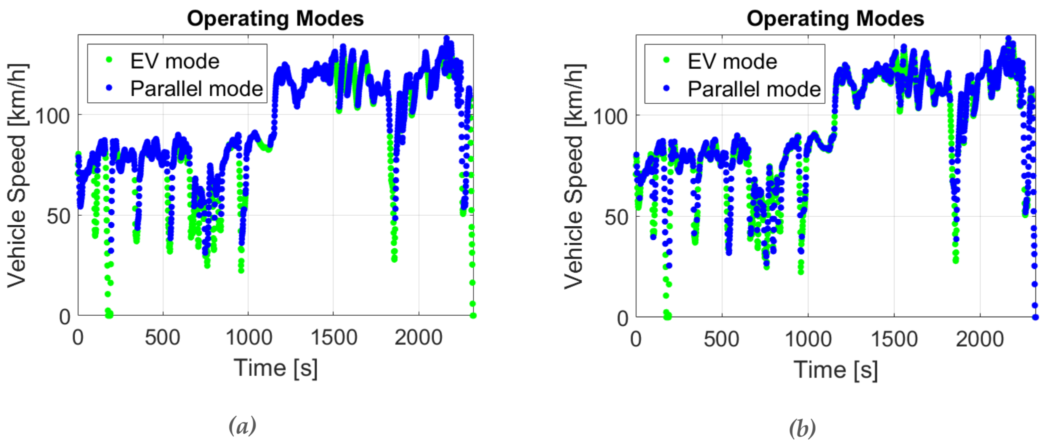

Figure 5.37 RDE operating modes with (a) Rule based strategy and (b) DP strategy

Figure 5.37 shows the RDE operating points. Despite the absence of external control, the operating modes seem to be similar in both RB and DP strategies. In both cases, the vehicle operates in Parallel mode with high vehicle speed while it is in EV at low speed, which is expected because in these conditions the power actuators are more efficient.

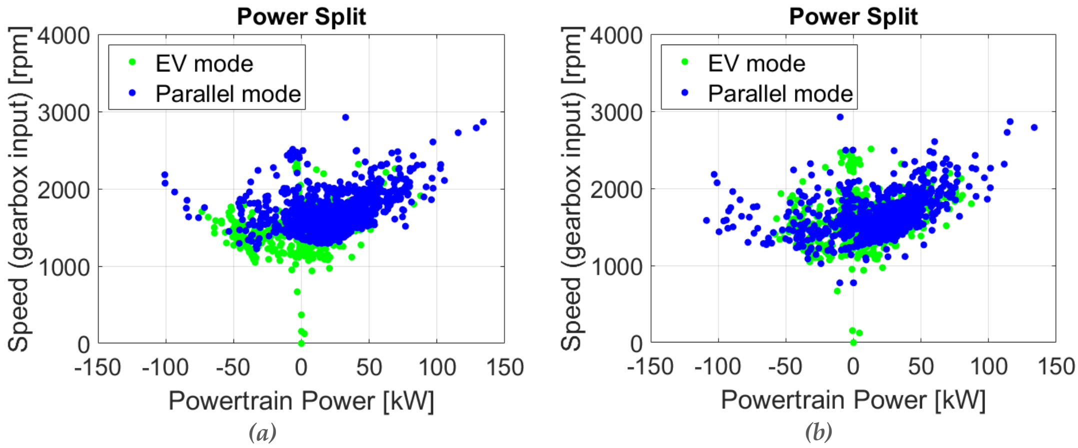

Figure 5.38 RDE power split with (a) Rule based strategy and (b) DP strategy

The power split performed by the DP is not consistent with the one obtained with NEDC and WLTC. As it is possible to see in Figure 5.39, the EM provides negative power for most of the time to charge the battery to obtain the CS, while the ICE drives the vehicle.

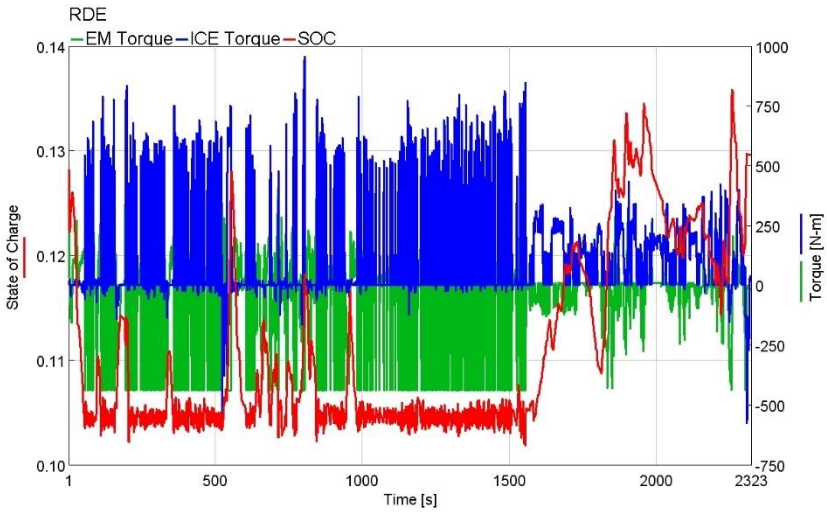

Figure 5.39 RDE driving cycle analysis

The global optimal solution is theoretically possible but practically infeasible due to the impossibility to extract a set of rules that can be performed on a real vehicle.

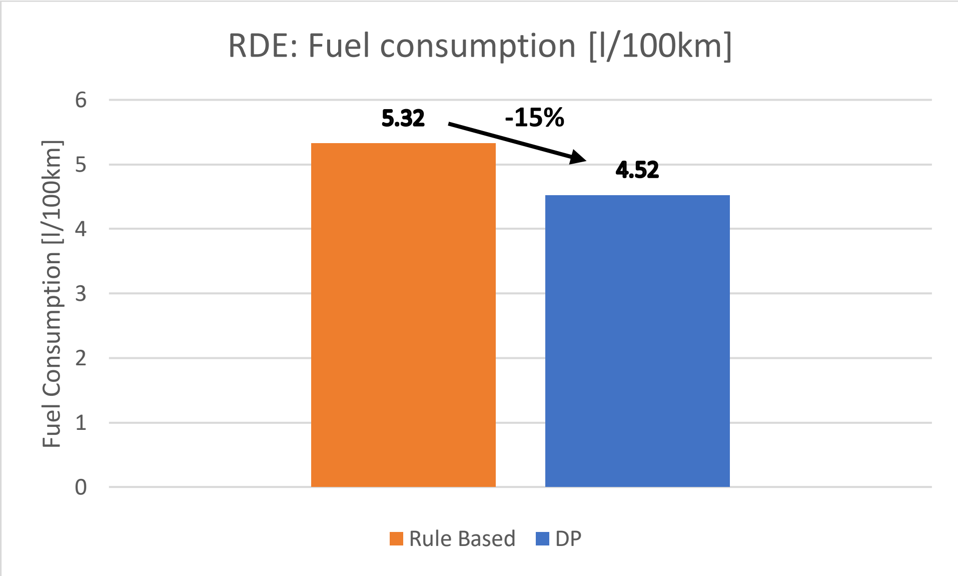

Figure 5.40 RDE: Fuel consumption

Although the RDE does not allow the external control on the ICE, the DP routine also assures, in this case, the fuel consumption reduction and so a reduction on CO_2 emissions. Figure 5.40 shows the fuel consumption reduction during the RDE that amounts to 15%.

6 Conclusions

The persistent environmental and climate challenge at European and global scales are driving the Government's policies towards long-term sustainability policies. Europe's transport sector, as one of the key economic sector, has a principal role in the reduction of environmental and climate pressures. In the past decades, the progressively stricter European regulations drove the automotive sectors to develop electrified vehicle technologies. In this context, the Hybrid Electric Vehicle represents the best compromise considering realistic economic, infrastructural and customer acceptance constraints.

However, differently from the conventional and electric vehicles with one power actuator, the HEVs are characterized by two or more sources of power, causing the increment of the powertrain complexity. A hybrid vehicle mandatory requires the introduction of an additional control layer, the Energy Management System, that decide the power split among the actuators. Hence, the benefits provided by the hybridization can be fully exploited only by an ad hoc powertrain control strategy. There are several energy management control strategies for this purpose proposed in literature. Among them, Dynamic Programming is the one that gives the global optimal energy management strategy.

The dissertation was focused on the optimization of the energy management system of a P2 Diesel Plug-In Hybrid Electric Vehicle (PHEV) already available on the market. The optimisation has been performed adopting the DP, in order to point out information which can be used to define new control laws to integrate with the Rule Based strategy adopted by the manufacturers. The software used for implementing the DP routine is GT-SUITE, a tool developed by Gamma Technology. To enable the DP, a kinematic model of the PHEV has been performed. Once the GT model has been validated, the DP has been applied on the NEDC, WLTC and RDE driving cycles. The backward kinematic optimisation results have been compared with experimental data achieved with the Rule Based strategy utilised on the real vehicle.

On the NEDC and WLTC driving cycles, an external controller has been imposed to switch off the ICE during deceleration phases to avoid unrealistic behaviour even if more convenient from a global optima perspective. Comparing the RB and DP strategies, it turns out that the adopted logics are very similar, however, the DP routine provide a significant enhancement of the vehicle fuel economy. It has been proved that adopting simple rules in the RB strategy, it is possible to obtain a reduction of fuel consumption and so of CO_2 emissions of almost 10%.

The GT-SUITE embedded DP does not allow to perform the external controller on the ICE to the RDE due to high computation effort that a real driving cycle involved. The DP provides infeasible results since it is impossible to extract a set of rules that can be performed on a real vehicle. Despite this, the DP results in present better behaviour from a fuel consumption perspective. Even in this case, the fuel reduction is in the order of 10%.

Acknowledgement

First of all, I would like to thanks my supervisors, Luciano and Luca, for allowing me to work on this exciting subject. Although the thesis work was done completely remotely, they were always available to support me both from a technical and human point of view.

I must thank my parents for helping me overcome the obstacles of this path and for enjoying my successes. I thank my older sisters Alessandra and Francesca for always being an example of strength and courage.

Thanks to my fellow of this adventure, the group of "New Energy", they have been a reference to me, and they have given me powerful motivation. Having friends like them was a great fortune for me.

A big hug goes to my friends Camilla, Francesca C., Francesca D., Giulia, Marica, Silvia and Vittoria for always being a constant presence in my life. What I am now and all my successes are thanks to them.

I would like to show gratitude to Linda and Lorenza to be a friend I can count on. Despite our diversity, our bond is indissoluble.

Finally, I want to thanks to Davide, my boyfriend and my colleague, for sharing with me these last years. His support and love are essential to me. Having a person to share everything with, with whom to look in the same direction is invaluable.

Bibliography

[1] European Commission, “Climate change consequences | Climate Action.” https://ec.europa.eu/clima/change/consequences_en (accessed Oct. 26, 2020).

[2] P. István, “The European environment-state and outlook 2020. Knowledge for transition to a sustainable Europe,” *Teruleti Statisztika*, vol. 60, no. 3. pp. 391–394, 2020, doi: 10.15196/TS600305.

[3] EEA, “Electric vehicles from life cycle and circular economy perspectives - TERM 2018: Transport and Environment Reporting Mechanism (TERM) report,” no. 13. p. 74 pp., 2018.

[4] L. Rolando, “An innovative methodology for the development of HEVs energy management,” 2012.

[5] EEA, “Progress of EU transport sector towards its environment and climate objectives.” https://www.eea.europa.eu/themes/transport/term/term-briefing-2018 (accessed Oct. 27, 2020).

[6] EEA, “Monitoring CO2 emissions from passenger cars and vans in 2013,” no. 19. p. 56, 2014, doi: 10.2800/23352.

[7] L. Rolando, “Hybrid Propulsion System – Energetic PhD Course.” Politecnico di Torino, 2019.

[8] IEA, “Global EV Outlook 2020.” 2020, doi: 10.1787/d394399e-en.

[9] EEA, “Emissions of air pollutants from transport.” https://www.eea.europa.eu/data-and-maps/indicators/transport-emissions-of-air-pollutants-8/transport-emissions-of-air-pollutants-8 (accessed Oct. 18, 2020).

[10] EEA, “Transport: increasing oil consumption and greenhouse gas emissions hamper EU progress towards environment and climate objectives.” https://www.eea.europa.eu/themes/transport/term/increasing-oil-consumption-and-ghg (accessed Oct. 18, 2020).

[11] Peter Mock, “2020–2030 CO2 standards for new cars and light-commercial vehicles in the European Union,” *ICCT*, no. October. pp. 1–19, 2017.

[12] EEA, “Explaining road transport emissions. A non-technical guide,” *European Environment Agency*. pp. 1–31, 2016, doi: 10.2800/71804.

[13] H. van Essen, M. Verbeek, S. Aarnink, and R. Smokers, “Assessment of the Modalities for LDV CO2 Regulations beyond 2020,” *CE Delft*, no. January 2017, p. 15, 2017, [Online]. Available:

https://ec.europa.eu/clima/sites/clima/files/transport/vehicles/docs/ldv_co2_modalities_for_regulations_beyond_2020_en.pdf.

[14] L. Rolando, “Fuel Consumption , CO2 and NOx Emissions of Rules for the Report,” no. x, 2020.

[15] M. Tutuianu *et al.*, “Development of a World-wide Worldwide harmonized Light duty driving Test Cycle,” *Tech. Rep.*, vol. 03, no. January, pp. 7–10, 2014.

[16] E. G. Giakoumis and A. T. Zachiotis, “Investigation of a diesel-engined vehicle’s performance and emissions during the WLTC driving cycle - Comparison with the NEDC,” *Energies*, vol. 10, no. 2, 2017, doi: 10.3390/en10020240.

[17] P. Mock, “Real-Driving Emissions Test Procedure for Exhaust Gas Pollutant Emissions of Cars and Light Commercial Vehicles in Europe,” *ICCT*, no. January. pp. 1–10, 2017.

[18] S. Onori, L. Serrao, and G. Rizzoni, “Hybrid electric vehicles: Energy management strategies,” *SpringerBriefs in Control, Automation and Robotics*, no. 9781447167792. pp. 1–112, 2016, doi: 10.1007/978-1-4471-6781-5.

[19] V. Due and V. Mild, “Classification of Hybrid Electric Vehicles,” no. 2017, pp. 6–8, 2020.

[20] D. Villa, “Investigation of hybrid powertrain architectures with focus on customer relevant conditions.” Politecnico di Torino.

[21] L. Rolando, “Hybridization as Enabler of New Engine Technologies,” 2020.

[22] M. Weiss, “Consistent Electrification of the Powertrain in Mercedes-Benz Cars – from Micro Hybrid to Plug-In,” *Int. Wiener Mot.*, 2010.

[23] M. F. Tansini, A., Fontaras G., Scassa M., DiPierro, G., “An Integrated Experimental and Numerical Methodology for Plug-In Hybrid Electric Vehicle 0D Modelling,” *SAE Tech. Pap.*, 2019.

[24] H. Sagha, “Modeling and Design of a NOx Emission Reduction Strategy for Lightweight Hybrid Electric Vehicles,” pp. 334–339, 2009.

[25] F. Millo *et al.*, “Analysis of Different Energy Management Strategies for Complex Hybrid Electric Vehicles,” vol. 11, pp. 1–12, 2014, doi: 10.3722/cadaps.2013.xxx-yyy.

[26] D. Bianchi *et al.*, “A rule-based strategy for a series/parallel hybrid electric vehicle: An approach based on dynamic programming,” *ASME 2010 Dyn. Syst. Control Conf. DSCC2010*, vol. 1, pp. 507–514, 2010, doi: 10.1115/DSCC2010-4233.

[27] G. Dipierro, F. Millo, M. Scassa, and A. Perazzo, “An Integrated Methodology for 0D Map-Based Powertrain Modelling Applied to a 48 v

Mild-Hybrid Diesel Passenger Car," *SAE Tech. Pap.*, vol. 2018-Septe, pp. 1–15, 2018, doi: 10.4271/2018-01-1659.

[28] F. Millo, L. Rolando, M. Andreata, and P. Torino, "Chapter Number Numerical Simulation for Vehicle Powertrain Development."

[29] L. Pulvirenti, "Development of an Equivalent Consumption Minimization Strategy (ECMS) for a High-Performance Hybrid Electric Vehicle," *Master thesis*. Politecnico di Torino, 2019.

[30] F. Millo, L. Rolando, and M. Andreat, "Numerical Simulation for Vehicle Powertrain Development," *Numer. Anal. - Theory Appl.*, 2011, doi: 10.5772/24111.

[31] D. D. Tran, M. Vafaeipour, M. El Baghdadi, R. Barrero, J. Van Mierlo, and O. Hegazy, "Thorough state-of-the-art analysis of electric and hybrid vehicle powertrains: Topologies and integrated energy management strategies," *Renew. Sustain. Energy Rev.*, vol. 119, p. 109596, 2020, doi: 10.1016/j.rser.2019.109596.

[32] L. Guzzella, "Vehicle Propulson Systems," *Foreign Affairs*, vol. 91, no. 5. pp. 1689–1699, 2012.

[33] B. Wnukowska, "Energy management in the industry," *Prz. Elektrotechniczny*, vol. 92, no. 2, pp. 125–128, 2016, doi: 10.15199/48.2016.02.35.

[34] Gamma Technologies, "Flow Theory Manual," 2020.

[35] Gamma Technologies, "User Manual." Gamma Technologies, 2020.

[36] G. DiPierro, E. Galvagno, G. Mari, F. Millo, M. Velardocchia, and A. Perazzo, "A Reverse-Engineering Method for Powertrain Parameters Characterization Applied to a P2 Plug-In Hybrid Electric Vehicle with Automatic Transmission," *SAE Tech. Pap. Ser.*, vol. 1, no. Lv, 2020, doi: 10.4271/2020-37-0021.